THE JOURNAL OF BIOLOGICAL CHEMISTRY VOL. 287, NO. 49, pp. 40956–40971, November 30, 2012

Human Sensory Neuron-specific Mas-related G Protein-coupled Receptors-X1 Sensitize and Directly Activate Transient Receptor Potential Cation Channel V1 via Distinct Signaling Pathways*

Received for publication, August 7, 2012, and in revised form, October 12, 2012 Published, JBC Papers in Press, October 16, 2012, DOI 10.1074/jbc.M112.408617

Hans Jürgen Solinski, Susanna Zierler, Thomas Gudermann, and Andreas Breit[1]

From the Walther-Straub-Institut für Pharmakologie und Toxikologie, Ludwig-Maximilians-Universität München 80336 München, Germany

Background: MRGPR-X1 are exclusively expressed in primary sensory neurons, provoke the sensation of pain, and are considered as promising targets for pain therapy.
Results: MRGPR-X1 sensitize TRPV1 for protons and heat via PKC and directly activate TRPV1 via DAG and PIP_2.
Conclusion: MRGPR-X1 modulate TRPV1 activity via multiple mechanisms.
Significance: Interrupting the functional interaction between MRGPR-X1 and TRPV1 is a promising approach to diminish pain.

Sensory neuron-specific Mas-related G protein-coupled receptors-X1 (MRGPR-X1) are primate-specific proteins that are exclusively expressed in primary sensory neurons and provoke pain in humans. Hence, MRGPR-X1 represent promising targets for future pain therapy, but signaling pathways activated by MRGPR-X1 are poorly understood. The transient receptor potential cation channel V1 (TRPV1) is also expressed in primary sensory neurons and detects painful stimuli such as protons and heat. G_q-promoted signaling has been shown to sensitize TRPV1 via protein kinase C (PKC)-dependent phosphorylation. In addition, recent studies suggested TRPV1 activation via a G_q-mediated mechanism involving diacylglycerol (DAG) or phosphatidylinositol-4,5-bisphosphate (PIP_2). However, it is not clear if DAG-promoted TRPV1 activation occurs independently from classic TRPV1 activation modes induced by heat and protons. Herein, we analyzed putative functional interactions between MRGPR-X1 and TRPV1 in a previously reported F11 cell line stably over-expressing MRGPR-X1. First, we found that MRGPR-X1 sensitized TRPV1 to heat and protons in a PKC-dependent manner. Second, we observed direct MRGPR-X1-mediated TRPV1 activation independent of MRGPR-X1-induced Ca^{2+}-release and PKC activity or other TRPV1 affecting enzymes such as lipoxygenase, extracellular signal-regulated kinases-1/2, sarcoma, or phosphoinositide 3-kinase. Investigating several TRPV1 mutants, we observed that removal of the TRPV1 binding site for DAG and of the putative PIP_2 sensor decreased MRGPR-X1-induced TRPV1 activation by 71 and 43%, respectively. Therefore, we demonstrate dual functional interactions between MRGPR-X1 and TRPV1, resulting in PKC-dependent TRPV1 sensitization and DAG/PIP_2-mediated activation. The molecular discrimination between TRPV1 sensitization and activation may help improve the specificity of current pain therapies.

Painful stimuli are detected at the peripheral terminals of primary sensory neurons. Thus, proteins expressed in these neurons and involved either in signal perception, propagation, or transmission are potential targets for pain therapy. Of particular interest are proteins that are highly enriched or exclusively expressed in primary sensory neurons, because specific modulation of these targets may allow circumvent untoward effects. Recently, Mas-related G protein-coupled receptors-X1 (MRGPR-X1)[2] have been shown to be exclusively expressed in primary sensory neurons and to be activated by bovine adrenal medulla peptide-8-22 (BAM8–22) originating from proteolytic cleavage of pro-enkephalin by pro-hormone convertases (1, 2). Several studies reported activation of the G_q pathway by MRGPR-X1 in overexpression systems (1, 3–5), and a recent study revealed increased pain sensation in 15 healthy volunteers after BAM8–22 application (6). In contrast, overexpression of MRGPR-X1 in rat dorsal root ganglia (DRG) neurons resulted in BAM8–22-mediated inhibition of voltage-gated calcium currents and activation of M-type potassium channels via $G_{i/o}$ proteins believed to blunt pain perception (7). Undoubtedly, MRGPR-X1 are involved in pain perception, but the underlying signaling pathways are still poorly defined.

The transient receptor potential cation channel V1 (TRPV1) is a non-selective ion channel that is expressed in primary sensory neurons and activated by capsaicin (CAP), heat, or protons (8, 9). Increased TRPV1 activity at the cellular level reliably correlates with enhanced pain perception. Inflammatory mediators like bradykinin (BK) potentiate heat- or proton-induced TRPV1 activity via phosphorylation of the channel protein by protein kinase A or C (PKC), calmodulin-dependent kinase II,

* This work was supported by Deutsche Forschungsgemeinschaft Grant BR 3346/3-1.
[1] To whom correspondence should be addressed. Tel.: 49-89-2180-75755; Fax: 49-89-2180-75721; E-mail: andreas.breit@lrz.uni-muenchen.de.

[2] The abbreviations used are: MRGPR-X1, Mas-related G protein-coupled receptors-X1; AUC, area under the curve; BAM, bovine adrenal medulla; BCTC, *N*-(4-tertiarybutylphenyl)-4-(3-cholorphyridin-2-yl)tetrahydropyrazine-1(2H)-carbox-amide; BIM-X, bisindolylmaleimide-X; BK, bradykinin; B2R, bradykinin-2 receptor; CAP, capsaicin; DAG, diacylglycerol; DRG, dorsal root ganglia; GPCR, G protein-coupled receptor; HBS, HEPES-buffered saline; LOX, lipoxygenase; NDGA, nordihydroguaiaretic acid; OAG, 1-oleoyl-2-acetyl glycerol; PIP_2, phosphatidylinositol 4,5-bisphosphate; PKD, protein kinase D; RT, room temperature; SRC, sarcoma kinase; TRPV1, transient receptor potential cation channel V1; pF, picofarads; PLC, phospholipase C.

phosphoinositide 3-kinase (PI3K), sarcoma kinase (SRC), or extracellular signal-regulated kinases-1/2 (ERK-1/2) (10–15). However, *bona fide* activation of TRPV1 caused by phosphorylation has been questioned (16, 17). In contrast, release of the phospholipase C (PLC) product diacylglycerol (DAG) has been suggested to enhance TRPV1 activity via binding to the channel protein (18) and degradation of the PLC substrate phosphatidylinositol-4,5-bisphosphate (PIP_2) to relieve TRPV1 from inhibitory PIP_2 effects, thereby activating the ion channel (17, 19). Therefore, GPCR-mediated activation of PLC can modulate TRPV1 activity via several distinct mechanisms.

Because of its dominant role in pain perception and its versatile regulation by G protein-coupled receptors (GPCR), TRPV1 is a likely target of MRGPR-X1-induced signaling. Therefore, we investigated the effects of BAM8–22 on TRPV1 activity in F11 cells (rat DRG neurons x murine neuroblastoma cells) stably expressing MRGPR-X1. We show that BAM8-22 sensitizes TRPV1 to heat and protons in a PKC-dependent manner. However, BAM8–22/MRGPR-X1 signaling also results in TRPV1 activation at room temperature (RT) and neutral pH. TRPV1 activation via MRGPR-X1 is independent of PKC activity or other TRPV1 modulating enzymes such as lipoxygenase (LOX), PI3K, ERK-1/2, protein kinase D (PKD), and SRC. In contrast, a TRPV1 mutant (TRPV1-Y511A) lacking the binding site for DAG displayed a 71% reduction in BAM8–22-promoted TRPV1 activation, suggesting that DAG production is involved in MRGPR-X1-dependent TRPV1 activation. Likewise, removal of amino acids 777–820 supposedly encompassing the TRPV1 sensor for PIP_2 (19) decreased BAM8-22-induced activation by 43%, whereas the double mutant (TRPV1-Y511A-δ777–820) was fully resistant to MRGPR-X1-mediated channel activation. Thus, we established the TRPV1 as an important downstream effecter of MRGPR-X1-promoted signaling, which is modulated by PKC- and DAG/PIP_2-dependent mechanisms. Knowledge about the functional interactions between MRGPR-X1 and TRPV1 will increase our understanding of human pain perception and might help to improve our current pain therapy.

EXPERIMENTAL PROCEDURES

Materials—Ham's F-12 nutrient mixture, FBS, penicillin/streptomycin, PBS, trypsin/EDTA, G418, and hypoxanthine/aminopterin/thymidine supplement were purchased from Invitrogen. PromoFectin® was from PromoCell (Heidelberg, Germany). BSA, pluronic F-127, and poly-L-lysine were from Sigma, and fura2-acetoxymethyl ester was obtained from Fluka (Deisenhofen, Germany). Bisindolylmaleimide-X (BIM-X), 1-oleoyl-2-acetyl glycerol (OAG), and thapsigargin were from Sigma. DAG kinase inhibitor-2 and U-73122 were from Calbiochem. PD-184352, LY-294002, nordihydroguaiaretic acid (NDGA) and CID-755673 were from Enzo life science (Lörrach, Germany), and *N*-(4-tertiarybutylphenyl)-4-(3-cholorphyridin-2-yl)-tetrahydropyrazine-1(2*H*)-carbox-amide (BCTC) was from Biomol (Hamburg, Germany). PP-2 and BAM8–22 were purchased from Biotrend (Cologne, Germany), BK was from Sigma, and CAP was obtained from Fluka.

Eukaryotic Expression Vectors—The plasmid coding for the TRPV1-YFP fusion protein (20) and the corresponding point mutants TRPV1-S800A-YFP (21) or TRPV1-S502A-YFP (22) were kindly provided by Dr. Tim D. Plant (Institute for Pharmacology and Toxicology, Marburg, Germany). The generation of the plasmid coding for the TRPV1-Y511A-YFP was carried out using the QuikChange® site-directed mutagenesis kit (Agilent, Waldbronn, Germany) with TRPV1-YFP as template and appropriate sense and antisense oligonucleotides spanning the mutated triplet and 25 flanking nucleotides. The deletion construct TRPV1-δ777–820-YFP was made by PCR using TRPV1-YFP as the template and the following 5′-phosphorylated primer: 5′-GGAGGAGCTCAGGGTGCGC-3′, 5′-GGATCCCTTAAGCCAGAGG-3′. The double mutant TRPV1-Y511A-δ777–820-YFP was also constructed by site-directed mutagenesis with the TRPV1-δ777–820-YFP plasmid as template and the same sense and antisense oligonucleotides as for TRPV1-Y511A-YFP construction. All constructs were verified by DNA sequencing.

Cell Culture and Transfection—F11 cells stably expressing MRGPR-X1 were previously described (4) and cultured in Ham's F-12 nutrient mixture supplemented with 15% FBS, 2 mM L-glutamine, hypoxanthine/amitriptyline/thymidine supplement, G418 (250 μg/ml), penicillin (100 units/ml), and streptomycin (100 μg/ml). For transient expression, F11-MRGPR-X1 cells were cultured for 24 h and then transfected with the appropriate vectors using PromoFectin® according to the manufacturer's protocol.

Fura2-based Single Cell Ca^{2+} Imaging—48 h before the experiment, F11-MRGPR-X1 cells were seeded at a density of $4–6 \times 10^4$ cells on glass coverslips in 6-well plates coated with 0.1% poly-L-lysine. After 24 h, cells were transfected with 1 μg of the indicated TRPV1-YFP constructs. The next day cells were loaded with 5 μM fura2-acetoxymethyl ester in HEPES-buffered saline (HBS, 10 mM HEPES, 5 mM KCl, 1 mM $MgCl_2$, 140 mM NaCl, 0.1% glucose, and 2 mM $CaCl_2$ adjusted to pH 7.4 with 1 M NaOH) supplemented with 0.02% pluronic F-127. Coverslips were washed twice with HBS and placed in a recording chamber, and YFP fluorescence of single cells was detected (excitation, 485 nm; emission, 510 nm). Afterward, we performed Ca^{2+} imaging with the entire cell pool and distinguished based on the YFP expression Ca^{2+} signals of TRPV1 expressing (F11-MRGPR-X1/TRPV1) and non-expressing (F11-MRGPR-X1) cells. This way distinct cell pools were treated the same way. Of note, fura2 labeling of cells did not interfere with the detection of YFP-based fluorescence. Average transfection efficacy reached 30–50%, and around 20 cells per coverslip were measured. Cells were analyzed using a Polychrome 5000 monochromator (Till-Photonics, Gräfelfing, Germany) and an Andor charge-coupled device camera coupled to an inverted microscope (IX71, Olympus, Hamburg, Germany). Ca^{2+} binding to fura2 was determined by alternate excitation of the cells with 340 or 380 nm every 0.5 s and concomitant detection of fluorescence emission at 520 nm. Fura2 ratios (340/380) were normalized by defining the first ratio (0.5 s) measured as 100%. To measure Mn^{2+}-induced quenching of fura2 fluorescence, fura2 emission was measured after exciting with 360 nm in intervals of 0.25 s. Normalization was carried out by defining the first ratio (0.25 s) measured as 100%. All inhibitors (concentrations as indicated) or the corresponding carrier control were

preincubated for 30 min and present during the entire measurement. For temperature-induced TRPV1 activation, 500 μl of prewarmed HBS (~55 °C) was injected in 500 μl of buffer at RT. This injection led to a sudden temperature increase to ~42 °C that declined rapidly to RT within 20 s. F11-MRGPR-X1 cells did not react to this treatment in the absence of the TRPV1 (data not shown). Proton-induced TRPV1 activation was initiated by injection of 500 μl of HBS with a pH of 6.4 (Mn^{2+} quench) or 5.0 (Ca^{2+} imaging) to 500 μl of HBS leading to a decrease in pH from 7.4 to 6.9 or 6.2, respectively. Only TRPV1-expressing cells reacted to this treatment (data not shown). To quantify ligand-induced calcium signals, the area between the curve and the base line (100%) of single cells was determined and is given as area under the curve (AUC). To quantify actions of effective inhibitors, AUC values of F11-MRGPR-X1/TRPV1 cells were divided by those of F11-MRGPR-X1 cells. Ratios of untreated cells were set to 100%, and effects of chemical inhibitors were calculated as percentage. Similar, to determine the effects of TRPV1 mutations, AUC values of TRPV1 wild-type or mutant-expressing cells were divided by those of F11-MRGPR-X1 cells. The ratio of TRPV1 wild-type cells was set to 100%, and effects of TRPV1 mutations were calculated as percentage.

Patch Clamp Analysis—Recordings of whole-cell currents were performed in F11-MRGPR-X1 cells at RT using an EPC-10 amplifier and PatchMaster (HEKA, Lambrecht, Germany). Currents were provoked by a voltage ramp protocol spanning from −100 to +100 mV (50-ms duration, 0.5 Hz) starting from a holding potential of 0 mV. All measurements were corrected for a liquid junction potential of 10 mV. The standard extracellular solution was HBS (pH 7.40, 290 mosmol), and the intracellular solution contained the following: 120 mM cesium glutamate, 8 mM NaCl, 1 mM $MgCl_2$, 3.62 mM $CaCl_2$, 10 mM HEPES, 2 mM MgATP, 10 mM EGTA, 5 mM EDTA (pH 7.20, 290 mosmol). Agonists were applied by local superfusion using the pressure ejection system MPCU-3 (Lorenz, Katlenburg-Lindau, Germany). Whole-cell currents were extracted at ±60 mV, normalized to total cell capacitance, and plotted against time. Ligand-induced currents were calculated by subtracting currents measured at time points 60 s from those obtained at 150 s. These values were used for quantification and statistical analysis. IV relationships of representative single cells before (60 s) and at the end of ligand application (150 s) are shown.

Data Analysis—Data were analyzed using Prism4.0. Statistical significance of differences was assessed by two-tailed Student's *t* test (between two groups) or by one-way analysis of variance and Tukey's honest significance post-hoc test (between more than two groups).

RESULTS

MRGPR-X1- and B2R-promoted TRPV1 Sensitization in F11 Cells—F11 cells (rat DRG neurons x murine neuroblastoma cells) endogenously express pain-modulating GPCR such as the bradykinin-2 receptor (B2R) and are a widely accepted model system to investigate DRG-related signaling pathways (23–35). To explore functional interactions between the MRGPR-X1 and the TRPV1, we took advantage of a previously reported F11 cell pool (F11-MRGPR-X1 cells) that stably expresses MRGPR-X1 (4). We transiently expressed a TRPV1-YFP fusion protein in these cells (F11-MRGPR-X1/TRPV1) and performed fura2 imaging with single cells (for details see "Experimental Procedures"). B2R-mediated activation of PLC has been shown to sensitize ligand-induced TRPV1 activity via PKC-dependent phosphorylation (11, 21, 22, 36–39). Therefore, we analyzed BK-mediated sensitization of CAP-induced Mn^{2+} influx into F11-MRGPR-X1/TRPV1 cells. As expected, prestimulation of cells with BK significantly increased CAP-promoted Mn^{2+} influx in a PKC-dependent manner, indicative of TRPV1 sensitization (Fig. 1*A*).

Having shown that functional interactions between GPCR and TRPV1 can be analyzed reliably in F11-MRGPR-X1 cells, we next investigated the effects of BAM8–22 on TRPV1 activity. Similar to BK, the MRGPR-X1-selective agonist significantly enhanced CAP-induced Mn^{2+} influx into F11-MRGPR-X1/TRPV1 cells (Fig. 1*B*), indicating TRPV1 sensitization by MRGPR-X1. Pretreatment of cells with the specific PKC inhibitor BIM-X completely blocked BAM8–22-induced TRPV1 sensitization (Fig. 1*B*). Furthermore, we found that BAM8–22 also sensitized TRPV1 to protons (Fig. 1*C*) or heat (Fig. 1*D*) in a PKC-dependent manner, indicating that BAM8–22 sensitized all three modes of TRPV1 activation.

PKC-mediated TRPV1 phosphorylation at positions serine 502 or 800 is required for GPCR-mediated TRPV1 sensitization (22, 40). In line with this notion, BAM8–22 did not sensitize CAP-induced Mn^{2+}-influx in F11-MRGPR-X1 cells expressing either the TRPV1-S502A (Fig. 1*E*) or the TRPV1-S800A mutant (Fig. 1*F*), further corroborating the notion that MRGPR-X1 signaling sensitizes ligand-induced TRPV1 activity in a PKC-dependent manner.

MRGPR-X1-induced Direct TRPV1 Activation Is PKC-independent—Although TRPV1 sensitization to heat and protons via G_q-dependent PKC activation is widely recognized, less is known about the impact of G_q/PLC signaling on direct TRPV1 activation independently from increased temperature or proton concentrations. Thus, we analyzed the consequences of TRPV1 expression on BAM8–22-induced Mn^{2+} influx at RT and a constant pH of 7.4 in the absence of CAP (Fig. 2, *A* and *B*). We observed that BAM8–22-induced Mn^{2+} influx into F11-MRGPR-X1/TRPV1 cells was significantly enhanced when compared with F11-MRGPR-X1 cells. Because the enhanced BAM8–22-induced Mn^{2+} influx into F11-MRGPR-X1/TRPV1 cells was blocked by the specific TRPV1 inhibitor BCTC (41), direct TRPV1 activation by MRGPR-X1 is most likely responsible for this effect. Given the important role for PKC in MRGPR-X1-mediated TRPV1 sensitization, we assumed that PKC would also be involved in TRPV1 activation. However, blockade of PKC activity by BIM-X did not affect BAM8–22-induced TRPV1 activation (Fig. 2*C*), suggesting that, in contrast to MRGPR-X1-induced TRPV1 sensitization, direct activation of TRPV1 by MRGPR-X1 is independent from PKC activity.

To corroborate this assumption, we measured BAM8–22-induced Ca^{2+} signals in the presence or absence of TRPV1. As shown in Fig. 3*A*, averaged Ca^{2+} responses in F11-MRGPR-X1/TRPV1 cells (AUC 55,950 ± 1,800) were about 4.1-fold larger than those obtained in cells solely expressing MRGPR-X1

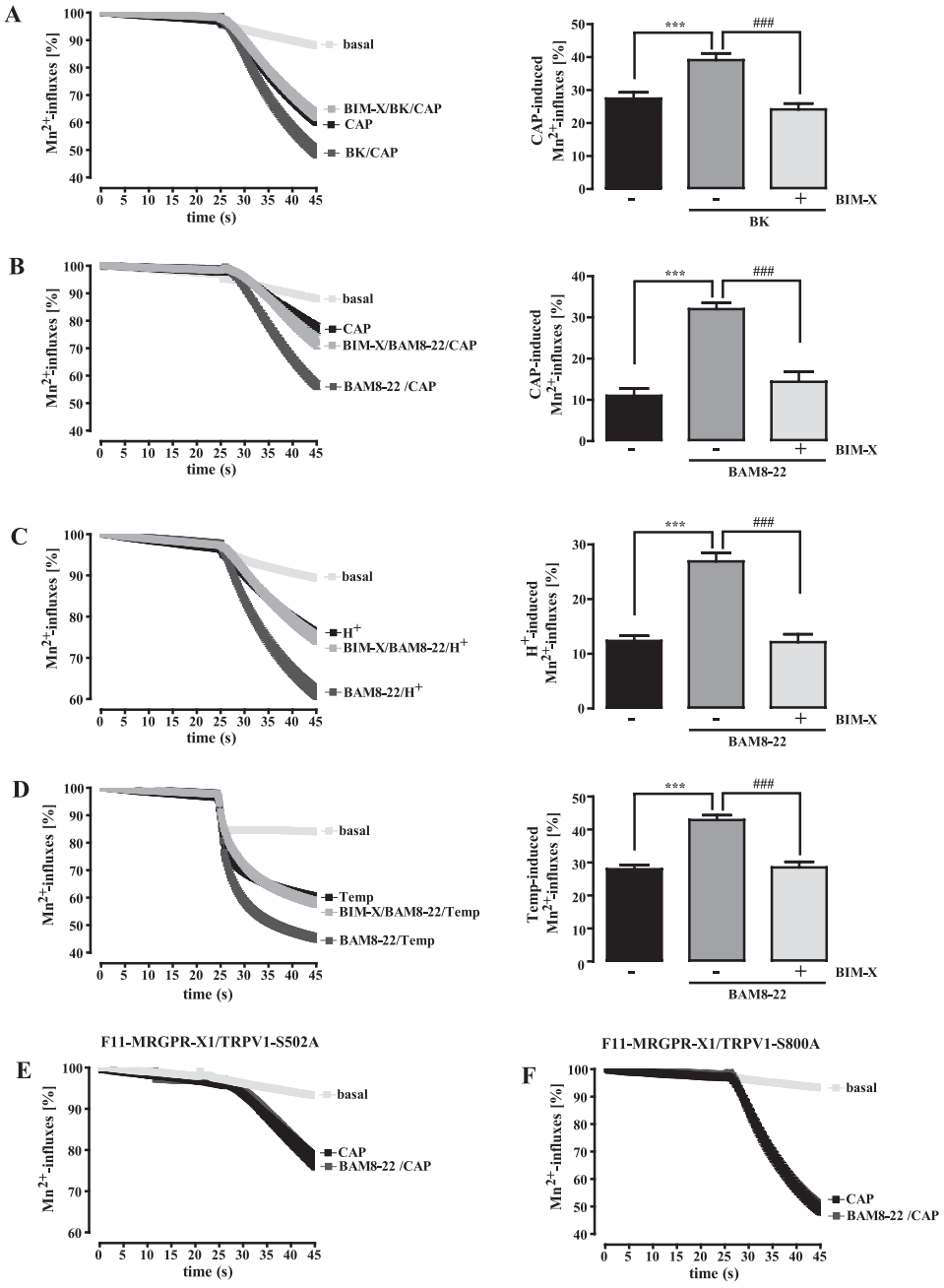

FIGURE 1. **MRGPR-X1- or B2R-induced TRPV1 sensitization is dependent on PKC activity.** Mn^{2+}-induced quenching of fura2 fluorescence in F11-MRGPR-X1/TRPV1 and F11-MRGPR-X1 cells (*A–D*) or in F11-MRGPR-X1 and TRPV1-S502A-YFP (*E*) or TRPV1-S800A-YFP (*F*) co-expressing F11-MRGPR-X1 cells was measured. CAP (5 nM, final) (*A*, *B*, *E*, and *F*), HCl (*C*), or pre-warmed buffer (*D*) were manually injected at time point 25 s; for details, see "Experimental Procedures." Cells were preincubated only with BK (100 nM, 5 min, *A*) or BAM8–22 (2 μM, 5 min, *B–F*) and either with the carrier DMSO (0.1%, 30 min, *A–D*) or with BIM-X (1 μM, 30 min, *A–D*) before TRPV1 activation. Data obtained from 3–5 independent experiments were compiled, normalized by defining the first value (0.25 s) measured as 100%, and expressed as the mean ± S.E. In *A–D* differences between basal and CAP-, proton-, or heat-provoked Mn^{2+}-induced quenching of fura2 fluorescence at time point 45 s are shown in *bar graphs*. *Asterisks* indicate a significant difference (***, $p < 0.001$) between basal and stimulated cells; *hash signs* (###, $p < 0.001$) indicate a significant difference between stimulated cells treated with either BIM-X or its carrier DMSO.

(AUC 10,900 ± 400) mostly due to prolonged Ca^{2+}-influx via TRPV1. Accordingly, BCTC abrogated enhanced Ca^{2+} signals in F11-MRGPR-X1/TRPV1 cells (Fig. 3*B*), indicating that direct activation of TRPV1 by MRGPR-X1 led to enhanced BAM8–22-induced Ca^{2+} influx. To investigate the role of PKC in this process, we either prestimulated F11-MRGPR-X1/TRPV1 cells with BIM-X or monitored BAM8–22-induced Ca^{2+} signaling in F11-MRGPR-X1 cells expressing TRPV1 mutants deficient of PKC phosphorylation sites. The PKC inhibitor had no effect on BAM8–22-induced Ca^{2+} signaling (Fig. 3*C*), and although both mutants were not sensitized by BAM8–22 (Fig. 1, *E* and *F*), they were robustly activated by MRGPR-X1 (Fig. 3, *D* + *E*), confirming that PKC-mediated phosphorylation is not involved in MRGPR-X1-induced TRPV1 activation. In conclusion, these data show that MRGPR-X1-promoted TRPV1 activation (PKC-independent) is mediated by distinct signaling pathways when compared with TRPV1 sensitization (PKC-dependent).

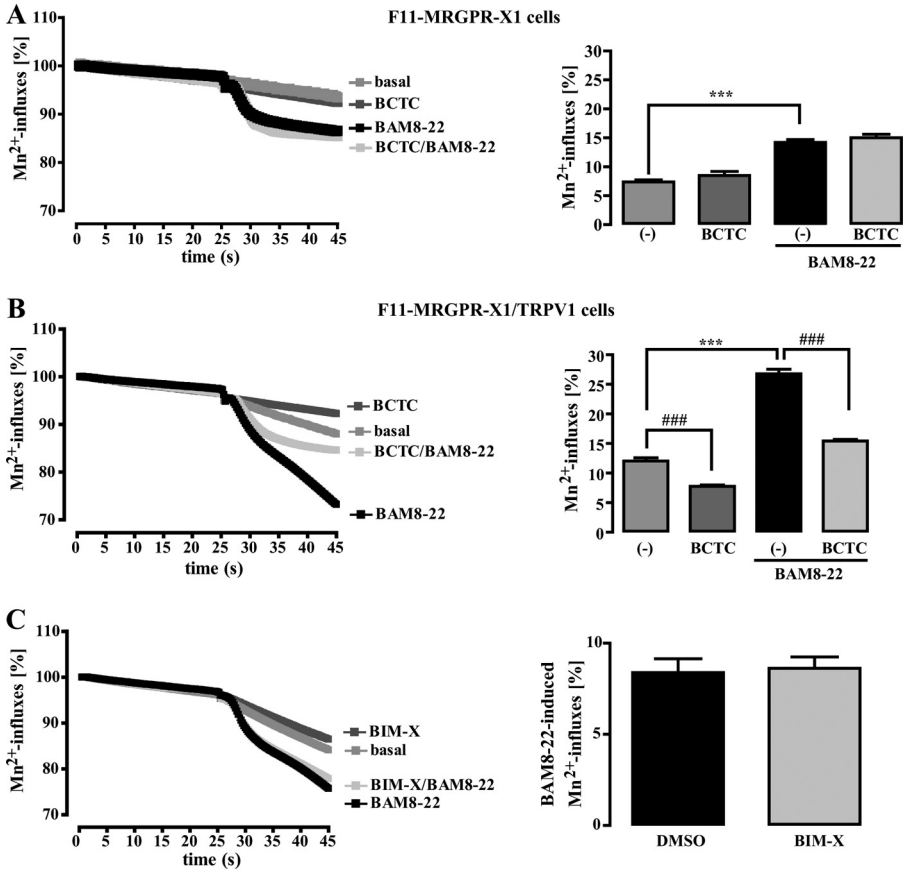

FIGURE 2. **MRGPR-X1-induced TRPV1 activation is independent from PKC activity (manganese influx).** Mn^{2+}-induced quenching of fura2 fluorescence in F11-MRGPR-X1 (*A*) or F11-MRGPR-X1/TRPV1 cells (*B* and *C*) were measured. BAM8–22 (2 μM, final) or HBS (basal) were manually injected at time point 25 s. In *A* and *B* cells were preincubated or not with BCTC (500 nM, 5 min), and in *C* cells were preincubated either with the carrier DMSO (0.1%, 30 min) or with BIM-X (1 μM, 30 min). Data from 3–5 independent experiments were compiled and normalized by defining the first value (0.25 s) measured as 100% and expressed as the mean ± S.E. In *A* and *B*, differences in Mn^{2+}-induced quenching of fura2 fluorescence before application and at time point 45 s are also shown in the *bar graphs*. In *C*, differences between basal (DMSO or BIM-X) and BAM8–22-provoked Mn^{2+}-induced quenching of fura2 fluorescence at time point 45 s are given. *Asterisks* indicate a significant difference (***, $p < 0.001$) between BAM8–22-stimulated and unstimulated cells; *hash signs* (###, $p < 0.001$) between BCTC-treated and untreated cells.

To substantiate our finding of PKC-independent TRPV1 activation, we performed whole-cell patch clamp experiments with TRPV1-YFP-transfected F11-MRGPR-X1 cells. As shown in Fig. 4*A*, after TRPV1 co-expression, 7 of 20 cells responded with inward (−26.6 ± 6.4 pA/pF) and outward (137.4 ± 28.8 pA/pF) currents to stimulation with 5 nM CAP. This ratio of responsive (TRPV1) to non-responsive cells (Mock) correlated well to the transfection efficacy of ~40% observed for the TRPV1-YFP plasmid. Furthermore, CAP-induced currents observed after TRPV1-YFP expression in F11-MRGPR-X1 cells displayed characteristic outwardly rectifying IV-relationships (Fig. 4*B*), indicating that these currents were mediated by the TRPV1 (42–44). Next, we measured whole-cell currents in TRPV1-YFP expressing F11-MRGPR-X1 cells after application of BAM8–22. As depicted in Fig. 4*C*, the MRGPR-X1 agonist induced inward (−24.6 ± 6.2 pA/pF) and outward (236.6 ± 58.1 pA/pF) currents in TRPV1-YFP-transfected cells that were blocked by BCTC and also exhibited a TRPV1-like IV relationship (Fig. 4*D*), indicating that MRGPR-X1 activation induced TRPV1 currents in F11-MRGPR-X1 cells at RT and neutral pH. To finally assess the role of PKC for MRGPR-X1-induced TRPV1 activation, we measured BAM8–22-induced currents in BIM-X pretreated cells (Fig. 4, *E* and *F*). Pharmacological PKC block did not affect BAM8–22-induced currents in TRPV1-expressing F11-MRGPR-X1 compared with DMSO-treated cells. Therefore, in congruence with data shown in Fig. 2 and 3, we provide conclusive evidence that direct TRPV1 activation via MRGPR-X1 in F11 cells is independent of PKC activity.

B2R-induced TRPV1 Activation Is Dependent on PKC and LOX Activity—Next, we wondered whether PKC-independent TRPV1 activation is unique for MRGPR-X1 or whether it would also apply to other established modulators of TRPV1 activity, such as BK. As shown in Fig. 5*A*, BK-induced Ca^{2+} signals in F11-MRGPR-X1 cells (AUC 9900 ± 700) were similar to those induced by BAM8–22 (Fig. 3*A*, AUC 10,900 ± 400), illustrating that activation of recombinant MRGPR-X1 did not elicit unphysiologically high Ca^{2+} transients compared with endogenously expressed B2R. Of note, BK-induced Ca^{2+} signals were 3.8-fold higher in F11-MRGPR-X1/TRPV1 cells (AUC 47,560 ± 3,500) when compared with F11-MRGPR-X1 cells (Fig. 5*A*), indicating direct TRPV1 activation also by B2R. However, blockade of PKC activity by BIM-X significantly reduced BK-induced Ca^{2+} signals by 53% (Fig. 5*C*) as compared with DMSO-treated cells (Fig. 5*B*). Thus, MRGPR-X1-induced TRPV1 activation is clearly distinct from MRGPR-X1-pro-

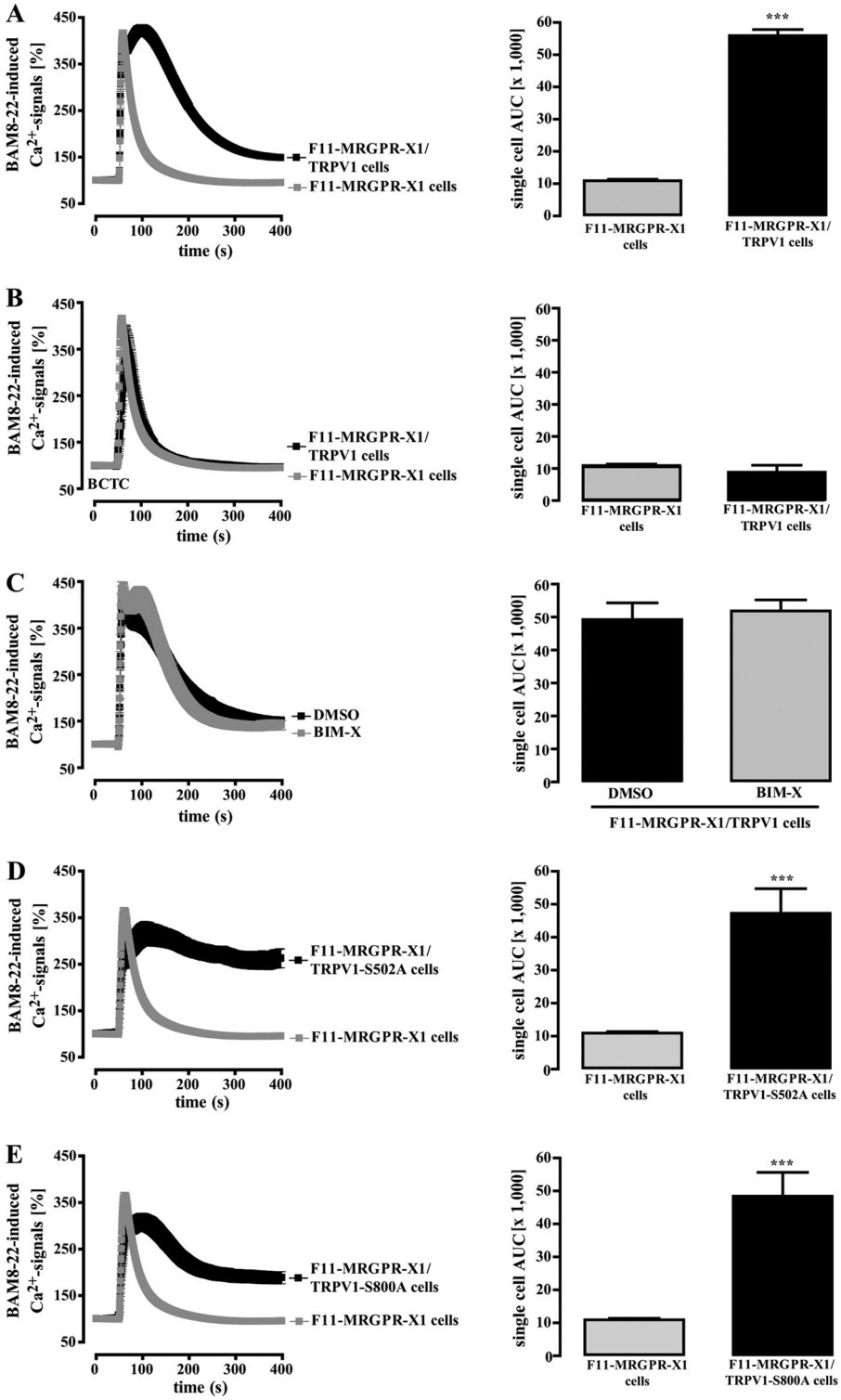

FIGURE 3. **MRGPR-X1-induced TRPV1 activation is independent from PKC activity (calcium signaling).** Ca^{2+} signals in fura2-loaded F11-MRGPR-X1 and F11-MRGPR-X1/TRPV1 cells (*A* and *B*), in F11-MRGPR-X1/TRPV1 cells (*C*), and in TRPV1-S502A-YFP (*D*) or TRPV1-S800A-YFP (*E*) co-expressing F11-MRGPR-X1 cells are shown. BAM8–22 (2 μM, final) was manually injected at time point 50 s. In *B*, cells were preincubated with BCTC (500 nM, 5 min), and in *C* cells were preincubated with BIM-X (1 μM, 30 min) or the carrier DMSO (0.1%, 30 min). Data from 3–5 independent experiments were compiled and normalized by defining the first value (0.5 s) measured as 100% and expressed as the mean ± S.E. The AUC for each measured cell was determined, and data of all cells were compiled, expressed as the mean ± S.E., and presented in *bar graphs*. *Asterisks* indicate a significant difference (***, $p < 0.001$) between TRPV1-YFP, TRPV1-S502A-YFP, or TRPV1-S800A-YFP co-expressing F11-MRGPR-X1 and F11-MRGPR-X1 cells.

moted TRPV1 sensitization and from TRPV1 activation mediated by B2R.

To lend more credibility to this hypothesis, we aimed to further compare BK- and BAM8–22-induced TRPV1 activation. LOX products such as 12-hydroperoxyeicosatetraenoic acid or *N*-arachidonoyl dopamine have also been shown to contribute to BK-mediated TRPV1 activation (45); thus, we used NDGA to block LOX activity. Because ethanol (ETOH) was used as

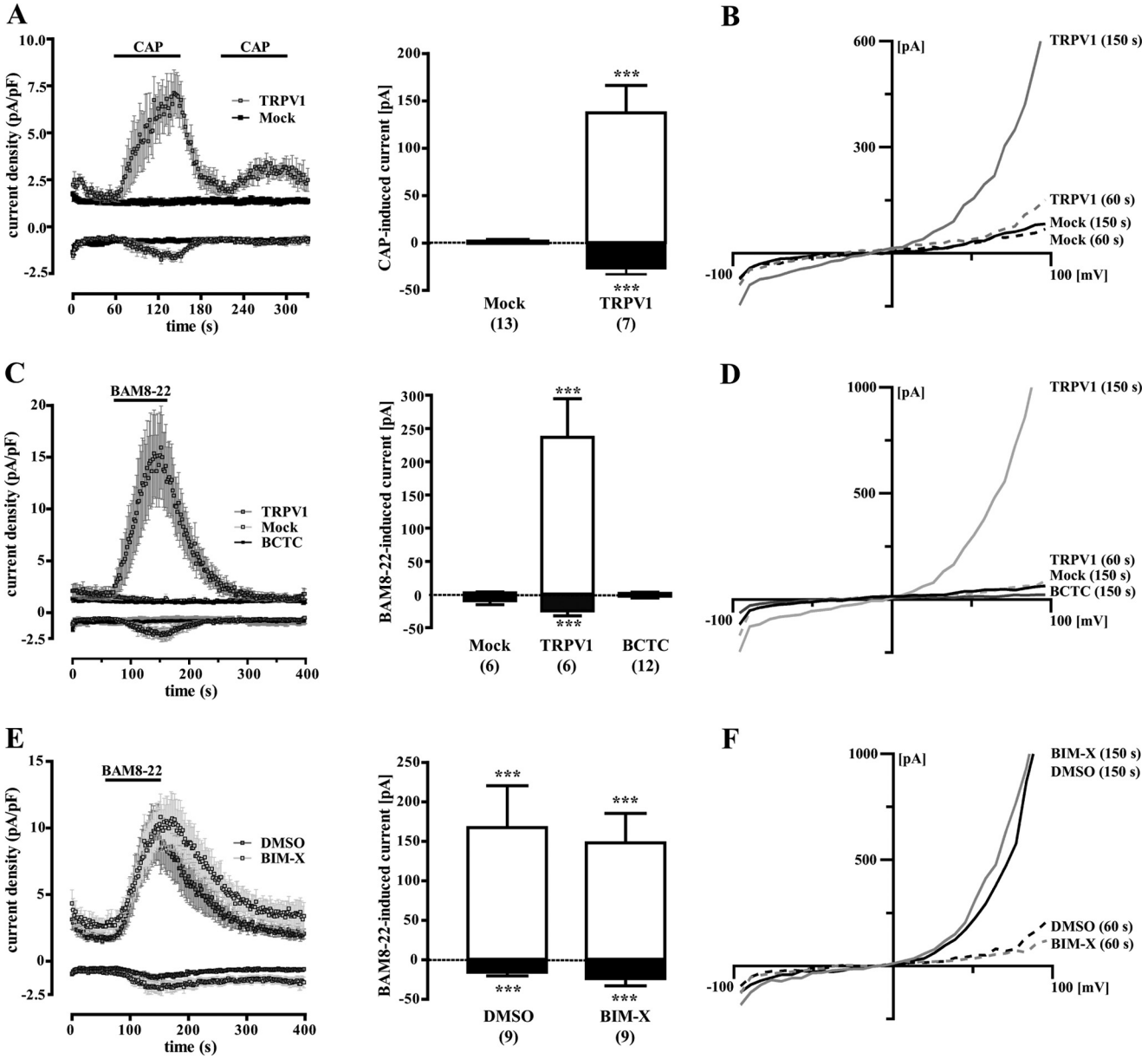

FIGURE 4. **MRGPR-X1-induced TRPV1 activation is independent from PKC activity (patch clamp analysis).** Averaged whole-cell current densities at ±60 mV were recorded in F11-MRGPR-X1 cells transfected with the TRPV1-YFP plasmid and stimulated with either 5 nM CAP (*A*) or 2 μM BAM8–22 (*C* and *E*), as indicated by the *black line above the traces*. Current densities of cells derived from 3–5 different transfections were compiled and are expressed as the mean ± S.E. Non-responding cells were defined as Mock cells, and responding cells were defined as TRPV1 cells. Ligand-induced currents at ±60 mV were calculated by subtracting the current before ligand application (60 s) from the current determined at the end of ligand application (150 s) and are presented in *bar graphs* (*white area* outward currents at +60 mV; *black area* inward currents at −60 mV). *Numbers in parenthesis* indicate the amount of cells analyzed. *Asterisks* indicate a significant difference (***, $p < 0.001$) between TRPV1 and Mock cells. In *C*, cells were also preincubated with BCTC (500 nM, final). In *E*, cells were either incubated with BIM-X (1 μM, 30 min) or the carrier DMSO (0.1%, 30 min). For each condition, typical IV relationships of single cells are shown in (*B*, *D*, and *F*). *pF*, picofarads.

a carrier for NDGA, we first analyzed the effects of ETOH on GPCR-induced TRPV1 activation. As shown in Fig. 6*A*, ETOH reduced the effects of TRPV1 co-expression on BK-induced Ca^{2+} signals, resulting in a mere 1.5-fold instead of a 3.8-fold increase as shown before (Fig. 5*A*) when compared with native F11-MRGPR-X1 cells. NDGA preincubation further decreased the effect of TRPV1 on BK-induced Ca^{2+} signals to 0.85-fold over F11-MRGPR-X1 cells, indicating that 44% of BK-induced TRPV1 activation required LOX activity in the presence of ETOH (Fig. 6*B*). In the case of BAM8–22, ETOH only slightly reduced TRPV1 effects on Ca^{2+} signaling, from 4.1 (Fig. 3*A*)- to 3.0-fold (Fig. 6*C*). In contrast, NDGA had no further significant effects on BAM8–22-induced TRPV1 activation (Fig. 6*D*), suggesting that LOX activity is involved in B2R- but not in MRGPR-X1-mediated TRPV1 activation.

MRGPR-X1-induced TRPV1 Activation Does Not Require Ca^{2+} Release, SRC, PI3K, PKD, or ERK-1/2 Activity—Given that MRGPR-X1-induced activation of TRPV1 does not require LOX or PKC activity, we addressed a putative role of SRC, PI3K, PKD, or ERK-1/2 in this process. As shown in Table 1, pharmacological inhibition of SRC, PI3K, PKD, or ERK-1/2 did not

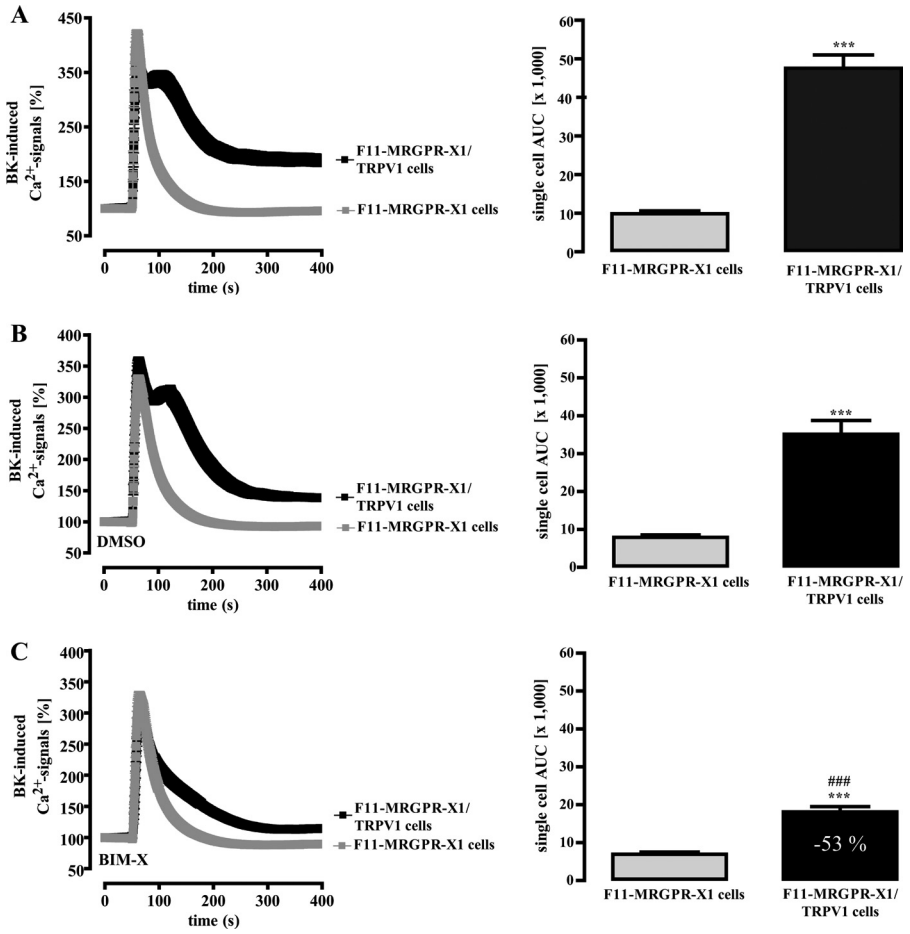

FIGURE 5. **B2R-induced TRPV1 activation is dependent on PKC activity.** Ca^{2+} signals in fura2-loaded F11-MRGPR-X1 or F11-MRGPR-X1/TRPV1 cells were monitored. BK (100 nM, final) was manually injected at time point 50 s. In *B*, cells were preincubated with the carrier DMSO (0.1%, 30 min), and in *C* cells were preincubated with BIM-X (1 μM, 30 min). Data from 3–5 independent experiments were compiled, normalized by defining the first value (0.5 s) measured as 100%, and expressed as the mean ± S.E. The AUC for each measured cell was determined, and data of all cells were compiled and expressed as the mean ± S.E. and presented in *bar graphs*. *Asterisks* indicate a significant difference (***, $p < 0.001$) between F11-MRGPR-X1/TRPV1 and F11-MRGPR-X1 cells; *hash signs* indicate a significant difference (###, $p < 0.001$) between BIM-X (*C*)- and DMSO (*B*)-treated F11-MRGPR-X1/TRPV1 cells.

significantly affect BAM8–22-induced TRPV1 activation, indicating that none of these kinases is involved. Therefore, we turned our attention toward PLC and its metabolites. The PLC inhibitor U-73122 abolished MRGPR-X1-mediated Ca^{2+} signals (Fig. 7*A*) in the absence or presence of TRPV1. To characterize the role of BAM8–22-induced Ca^{2+} release for TRPV1 activation, intracellular Ca^{2+} stores were depleted by pretreatment of cells with thapsigargin. Emptying of stores precluded BAM8–22-induced Ca^{2+} release in F11-MRGPR-X1 and F11-MRGPR-X1/TRPV1 cells, as illustrated by the loss of the rapid initial Ca^{2+} peak (Fig. 7*B*). However, BAM8–22 still elicited Ca^{2+} transients (AUC 26,400 ± 3,300) in F11-MRGPR-X1/TRPV1 cells, indicative of MRGPR-X1-dependent TRPV1 activation. Thus, we propose that MRGPR-X1-mediated Ca^{2+} release is not required for direct TRPV1 activation, thereby excluding Ca^{2+}-dependent proteins such as calmodulin-dependent kinase II as potential signaling intermediates linking MRGPR-X1 to TRPV1 activation.

MRGPR-X1-induced TRPV1 Activation Requires Binding Sites for DAG and PIP_2—Recent reports suggested that the PLC product DAG directly binds to and activates TRPV1. However, studies by others did not observe such interactions (18, 46). To assess the role of DAG in the regulation of TRPV1 activity in F11 cells, we employed a DAG kinase inhibitor to accumulate endogenous DAG. As shown in Fig. 8*A*, DAG kinase inhibition gave rise to long-lasting increases in $[Ca^{2+}]_i$ in F11-MRGPR-X1/TRPV1, but not in F11-MRGPR-X1 cells, suggesting that TRPV1 is activated by DAG in F11 cells. Furthermore, OAG, a cell-permeable DAG derivative, induced Ca^{2+} signals in F11-MRGPR-X1/TRPV1 but not in F11-MRGPR-X1 cells (Fig. 8*B*). Because OAG also activates PKCs, we preincubated cells with BIM-X to differentiate between a PKC-mediated and a direct OAG effect on TRPV1 activity. A saturating BIM-X concentration partially blocked OAG-induced TRPV1 activation (Fig. 8*C*), indicating that OAG affects TRPV1 activity in a PKC-dependent and -independent manner.

Recently, it has been shown that tyrosine 511 is involved in TRPV1 binding to CAP or OAG/DAG (18). However, Tyr-511 is not a part of the TRPV1 binding site for protons (47), and proton binding to the TRPV1 does not interfere with its binding to CAP (48). To investigate a role of Tyr-511 for TRPV1 activation by CAP, OAG, protons, BAM8–22, and BK, we replaced tyrosine 511 by an alanine (TRPV1-Y511A-YFP). As expected from previous data, the Y511A switch abrogated CAP-induced

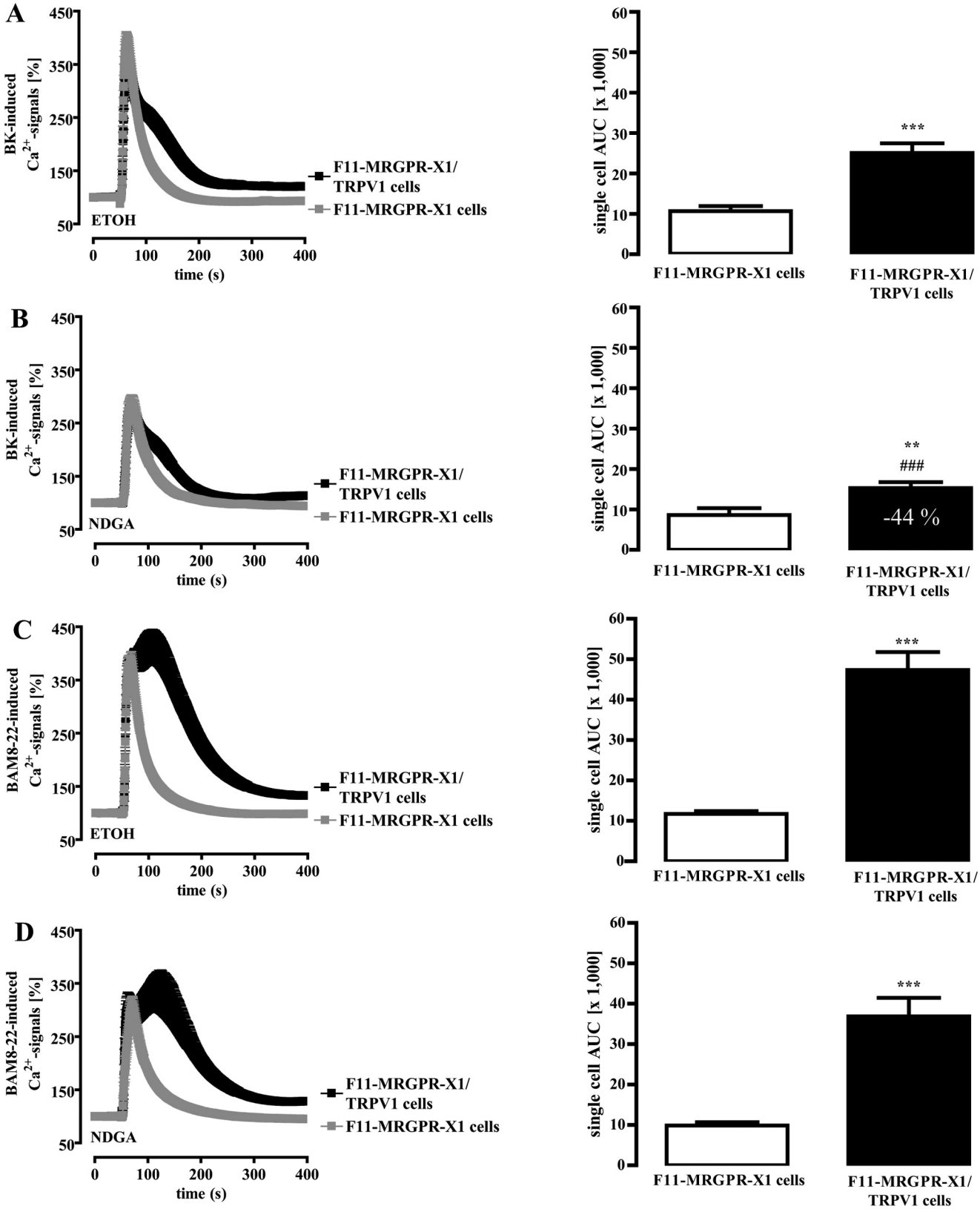

FIGURE 6. **LOX activity is required for B2R but not for MRGPR-X1-promoted TRPV1 activation.** Ca^{2+} signals in single fura2-loaded F11-MRGPR-X1 or F11-MRGPR-X1/TRPV1 cells were monitored. BK (100 nM, final) (*A* and *B*) and BAM8–22 (2 μM, final) (*C* and *D*) were manually injected at time point 50 s. Cells were preincubated with ETOH (0.1%, 30 min) (*A* and *C*) and NDGA (10 μM, 30 min) (*B* and *D*). Data from 3–5 independent experiments were compiled, normalized by defining the first ratio (0.5 s) measured as 100%, and expressed as the mean ± S.E. The AUC for each measured cell was determined, and data of all cells were compiled, expressed as the mean ± S.E. and presented in *bar graphs*. *Asterisks* indicate a significant difference (***, $p < 0.001$; **, $p < 0.01$) between F11-MRGPR-X1/TRPV1 and F11-MRGPR-X1 cells; *hash signs* indicate a significant difference (###, $p < 0.001$) between ETOH- and NDGA-treated F11-MRGPR-X1/TRPV1 cells stimulated with BK.

TABLE 1

SRC, PI3K, PKD, or ERK-1/2 activity is not required for MRGPR-X1-promoted TRPV1 activation

BAM8–22-induced Ca^{2+} signals in fura2-loaded F11-MRGPR-X1 and F11-MRGPR-X1/TRPV1 cells were measured and quantified by calculating the AUC (×1000) for each measured cell. Data from 3–5 independent experiments were compiled and expressed as the mean ± S.E. To block the activity of various kinases, cells were preincubated for 30 min with PP-2 (10 μM, SRC), LY-294002 (10 μM, PI3K), CID-755673 (1 μM, PKD), PD-184352 (10 μM, ERK-1/2), or the corresponding carrier control DMSO (0.1%). No significant difference between DMSO- and inhibitor-treated F11-MRGPR-X1 or F11-MRGPR-X1/TRPV1 cells were observed.

Cells	DMSO	PP-2	LY-294002	CID-755673	PD-184352
F11-MRGPR-X1	11.7 ± 0.9	15.9 ± 1.4	14.0 ± 1.8	10.7 ± 1.0	8.1 ± 0.6
F11-MRGPR-X1/TRPV1	47.0 ± 2.7[a]	55.2 ± 5.6[a]	56.2 ± 8.1[a]	56.0 ± 7.5[a]	40.8 ± 4.1[a]

[a] $p < 0.001$, significant differences between F11-MRGPR-X1 and F11-MRGPR-X1/TRPV1 cells.

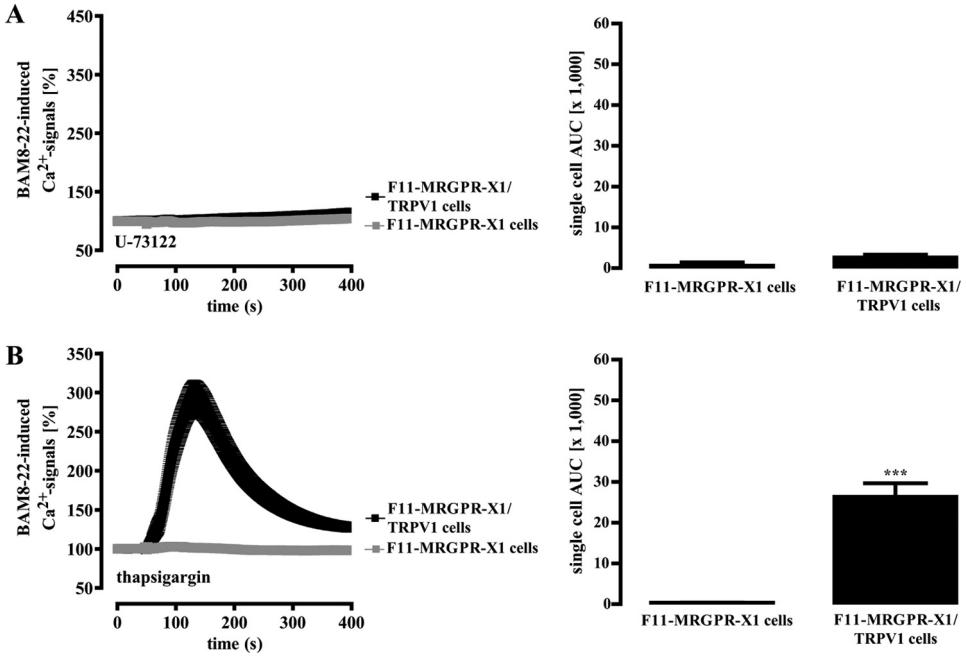

FIGURE 7. **MRGPR-X1-induced TRPV1 activation is independent from receptor-mediated calcium release.** Ca^{2+} signals in fura2-loaded F11-MRGPR-X1 or F11-MRGPR-X1/TRPV1 cells preincubated with U-73122 (10 μM, 30 min) (*A*) and with thapsigargin (1 μM, 30 min) (*B*) were monitored. BAM8–22 (2 μM, final) was manually injected at time point 50 s. Data from 3–5 independent experiments were compiled, normalized by defining the first value (0.5 s) measured as 100%, and expressed as the mean ± S.E. The AUC for each measured cell was determined, and data of all cells were compiled, expressed as the mean ± S.E., and presented in *bar graphs*. *Asterisks* indicate a significant difference (***, $p < 0.001$) between F11-MRGPR-X1/TRPV1, and F11-MRGPR-X1 cells.

(Fig. 9*A*) and drastically reduced OAG-dependent Ca^{2+} signals (Fig. 9*B*). However, the Y511A mutant and wild-type TRPV1 were similarly activated by protons (Fig. 9*C*), demonstrating that the Y511A variant was functionally expressed at the cell surface. Interestingly, enhancement of BAM8–22-induced Ca^{2+} signals in TRPV1-Y511A expressing F11-MRGPR-X1 cells were significantly reduced when compared with F11-MRGPR-X1/TRPV1 cells (Fig. 9*D*), suggesting that DAG is involved in MRGPR-X1-induced TRPV1 activation. As shown in Fig. 9*E*, BK-induced TRPV1 activation was nearly abolished in TRPV1-Y511A-expressing cells, indicating that besides PKC and LOX, DAG is also involved in B2R-mediated TRPV1 activation. However, although the exchange of tyrosine 511 to alanine diminished BAM8–22-induced TRPV1 activation, significant activation was still detectable.

The PLC substrate PIP_2 is supposed to inhibit TRPV1 activity (17). Therefore, PLC-mediated degradation of PIP_2 could also lead to MRGPR-X1-induced TRPV1 activation. Forty-three amino acid residues in the TRPV1 C terminus have been suggested to serve as the PIP_2 binding site (19). Thus, we constructed a mutant that lacks this portion of the TRPV1 protein (TRPV1-δ777–820-YFP) and, thus, is not inhibited by PIP_2 anymore, as indicated by slightly increased basal $[Ca^{2+}]_i$ in TRPV1-δ777–820-YFP compared with TRPV1-YFP expressing F11-MRGPR-X1 cells (data not shown). CAP-induced Ca^{2+} signals were indistinguishable between wild-type and TRPV1-δ777–820-expressing F11-MRGPR-X1 cells (Fig. 10*A*). In contrast, BAM8–22-induced TRPV1 activity was partially inhibited, suggesting that both DAG and PIP_2 are involved in MRGPR-X1-mediated TRPV1 activation (Fig. 10*B*). Notably, BK-induced TRPV1 activation was abrogated after removal of the PIP_2 binding site (Fig. 10*C*), illustrating that, in contrast to the situation with BAM8–22, BK effects on TRPV1 are nearly fully dependent on the PIP_2 binding site.

To definitively determine the impact of both DAG and PIP_2 on MRGPR-X1-mediated TRPV1 activation, we generated a double mutant that lacks the DAG binding site as well as the reported PIP_2 sensor (TRPV1-Y511A-δ777–820-YFP). This double mutant was still activated by protons (Fig. 11*A*), indicating that these modifications allowed proper folding and membrane translocation of a functional active channel protein. Of note, BAM8–22 activation was completely abolished (Fig. 11*B*), providing further evidence that both DAG production and PIP_2 degradation mediate BAM8–22-induced TRPV1 activation in F11-MRGPR-X1 cells.

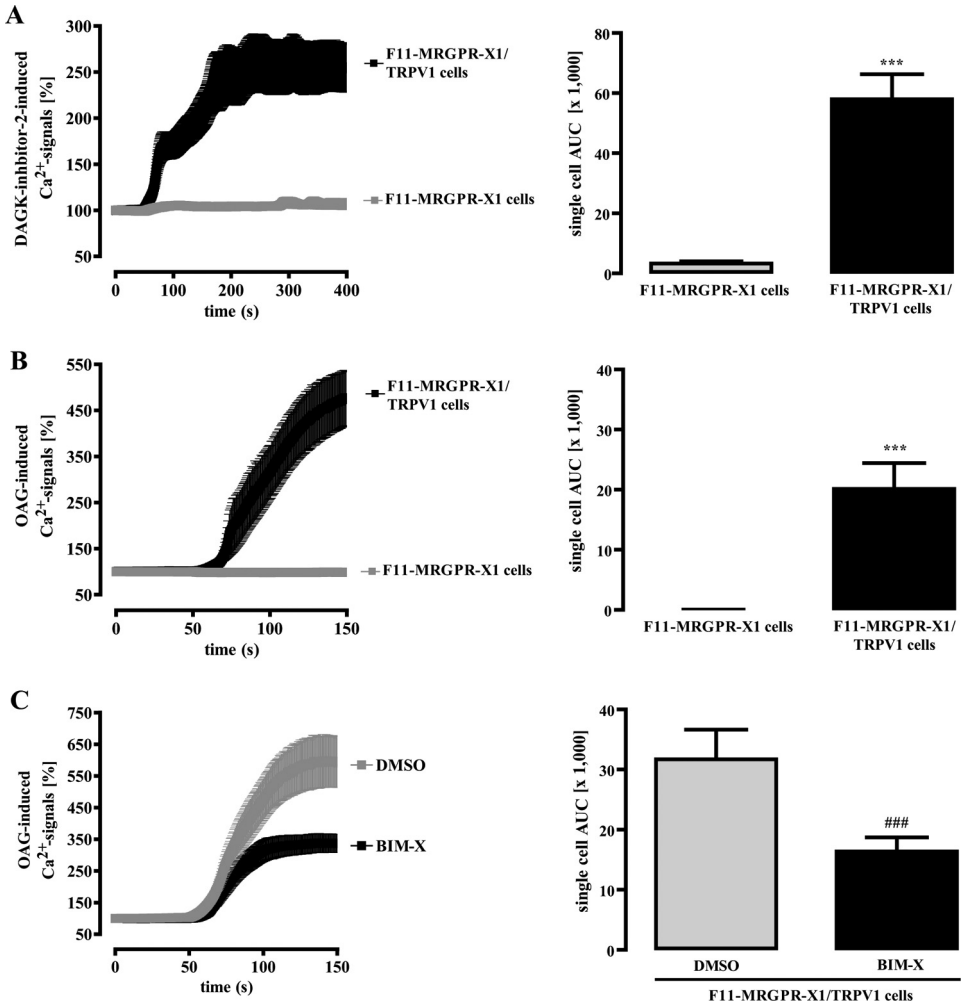

FIGURE 8. **DAG/OAG-induced TRPV1 activation in F11 cells.** Ca^{2+} signals in fura2-loaded F11-MRGPR-X1 or F11-MRGPR-X1/TRPV1 cells were monitored. DAG kinase (*DAGK*) inhibitor-2 (10 μM, final) (*A*) and OAG (100 μM, final) (*B* and *C*) were manually injected at time point 50 s. Cells were preincubated with BIM-X (1 μM, 30 min) (*A* and *C*) and a separate pool of cells with the carrier DMSO (0.1%, 30 min) (C). Data from 3–5 independent experiments were compiled, normalized by defining the first value (0.5 s) measured as 100%, and expressed as the mean ± S.E. The AUC for each measured cell was determined, and data of all cells were compiled, expressed as the mean ± S.E., and presented in *bar graphs*. *Asterisks* indicate a significant difference (***, $p < 0.001$) between F11-MRGPR-X1/TRPV1 and F11-MRGPR-X1 cells; *hash signs* indicate a significant difference (###, $p < 0.001$) between BIM-X- and DMSO-treated F11-MRGPR-X1/TRPV1 cells.

DISCUSSION

Due to the exclusive expression in DRG neurons, high affinity binding to pro-enkephalin cleavage products and their role for nociception in humans, MRGPR-X1 are considered as promising novel targets for pain therapy. Of note, MRGPR-X1 are primate-specific receptors (1, 2, 5, 49). In general, primate-specific genes are predominantly expressed in cells of the reproductive system or in neurons (50), and disease-causing genes are strongly enriched among primate-specific genes (51), highlighting their significance as therapeutic targets.

However, primate-specific expression is also a major impediment to functional analysis because of lack of suitable *in vivo* models and endogenous expression systems. Regarding the MRGPR-X1 subtype, one rodent receptor activated by BAM8–22 was identified in mice and rats (MRGPR-C) (1, 2). However, apart from common high affinity binding to BAM8–22, rodent MRGPR-C and human MRGPR-X1 exhibit fundamental differences in their affinity to other endogenous peptides, as previously reported (4, 52, 53). Furthermore, in contrast to rodent MRGPR-C, human MRGPR-X1 resist β-arrestin-dependent, agonist-promoted endocytosis (4), not only affecting signal duration but also directing GPCR-promoted signaling toward distinct signaling pathways (54). Therefore, we concur with other investigators in that the function of human MRGPR-X1 may not be accurately extrapolated from studies with rodent MRGPR-C (5, 7).

Herein, we used a recently established F11 cell line (rat DRG neurons x murine neuroblastoma cells) that stably expresses MRGPR-X1 (4) and analyzed their functional interactions with TRPV1. F11 cells emerged as a useful tool for the analysis of DRG-related signaling pathways, and several studies pointed out striking similarities between F11 cells and cultured DRG neurons (23–35). In this vein, molecular mechanisms underlying B2R-dependent signaling to TRPV1 in DRG neurons, *i.e.* sensitization by PKC or activation by PIP_2 degradation, were also observed in F11-MRGPR-X1 cells. Because Ca^{2+} transients initiated by endogenously expressed B2R and recombinant MRGPR-X1 were

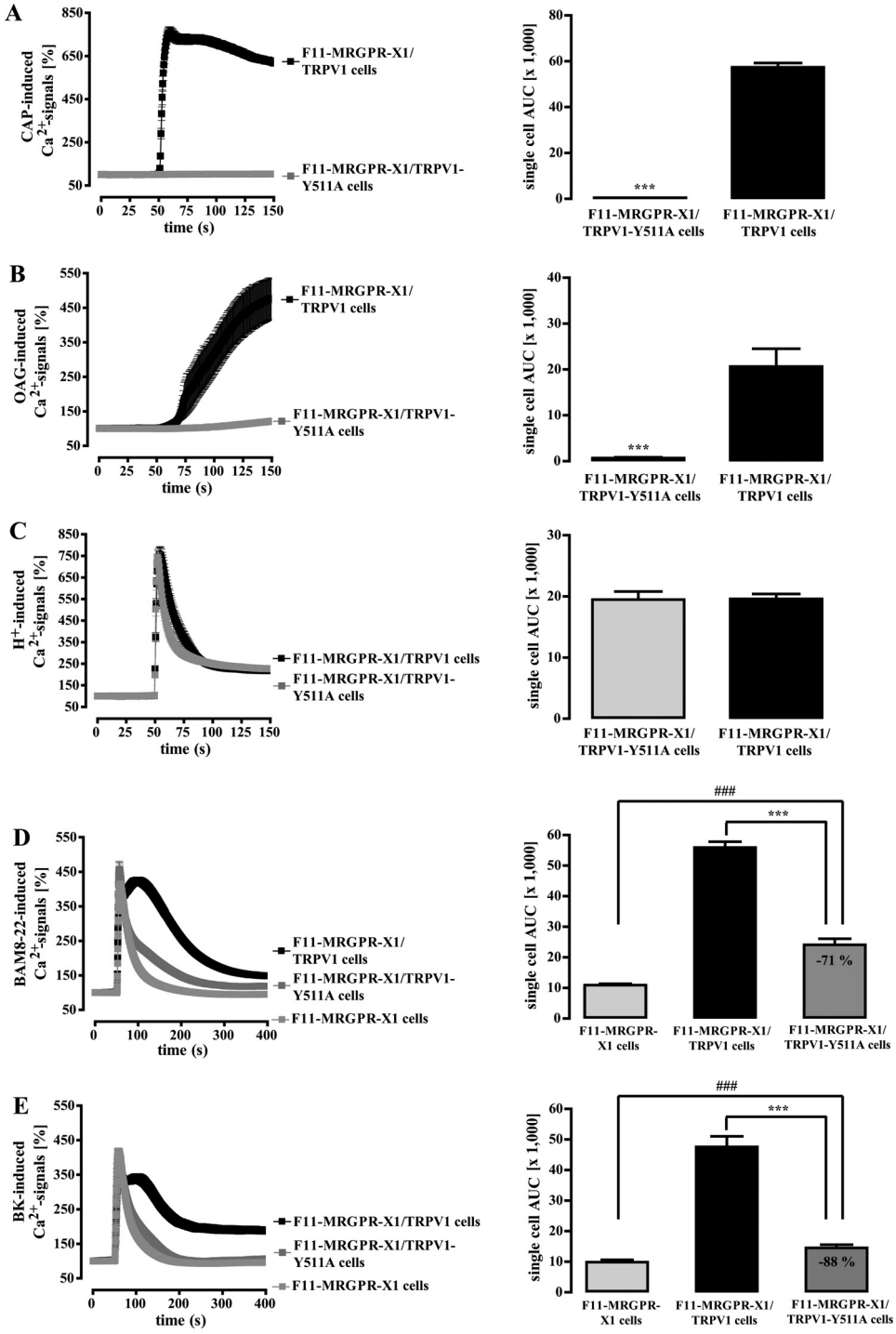

FIGURE 9. **MRGPR-X1-induced TRPV1 activation requires the DAG binding site of the TRPV1.** Ca^{2+} signals in fura2-loaded F11-MRGPR-X1 cells and TRPV1-YFP or TRPV1-Y511A-YFP co-expressing F11-MRGPR-X1 cells were monitored. CAP (10 nM, final) (*A*), OAG (100 μM, final) (*B*), HCl (pH 5.0) (*C*), BAM8–22 (2 μM, final) (*D*), and BK (100 nM, final) (*E*) were manually injected at time point 50 s. In *B* cells were preincubated with BIM-X (1 μM, 30 min) to avoid the effects of OAG on TRPV1 activity due to PKC-dependent TRPV1 phosphorylation (see Fig. 8*C*). Data from 3–5 independent experiments were compiled, normalized by defining the first value (0.5 s) measured as 100%, and expressed as the mean ± S.E. The AUC for each measured cell was determined, and data of all cells were compiled, expressed as the mean ± S.E., and presented in *bar graphs*. *Asterisks* (***, $p < 0.001$) indicate a significant difference between TRPV1-Y511A-YFP co-expressing F11-MRGPR-X1 and F11-MRGPR-X1/TRPV1 cells; *hash signs* (###, $p < 0.001$) indicate a significant difference between F11-MRGPR-X1 and TRPV1-Y511A-YFP co-expressing F11-MRGPR-X1 cells.

comparable, we consider F11-MRGPR-X1 cells as a reliable model system to investigate functional interactions between TRPV1 and human MRGPR-X1.

Using an established PKC inhibitor and two TRPV1 mutants lacking serine residues required for PKC-mediated TRPV1 sensitization, we show that MRGPR-X1 sensitize the TRPV1 in a PKC-dependent manner. Thus, we assign the human MRGPR-X1 to the large group of G_q-coupled receptors that sensitize nociceptors to the "inflammatory soup" via PKC-dependent mechanisms (11, 21, 22, 36–39, 42).

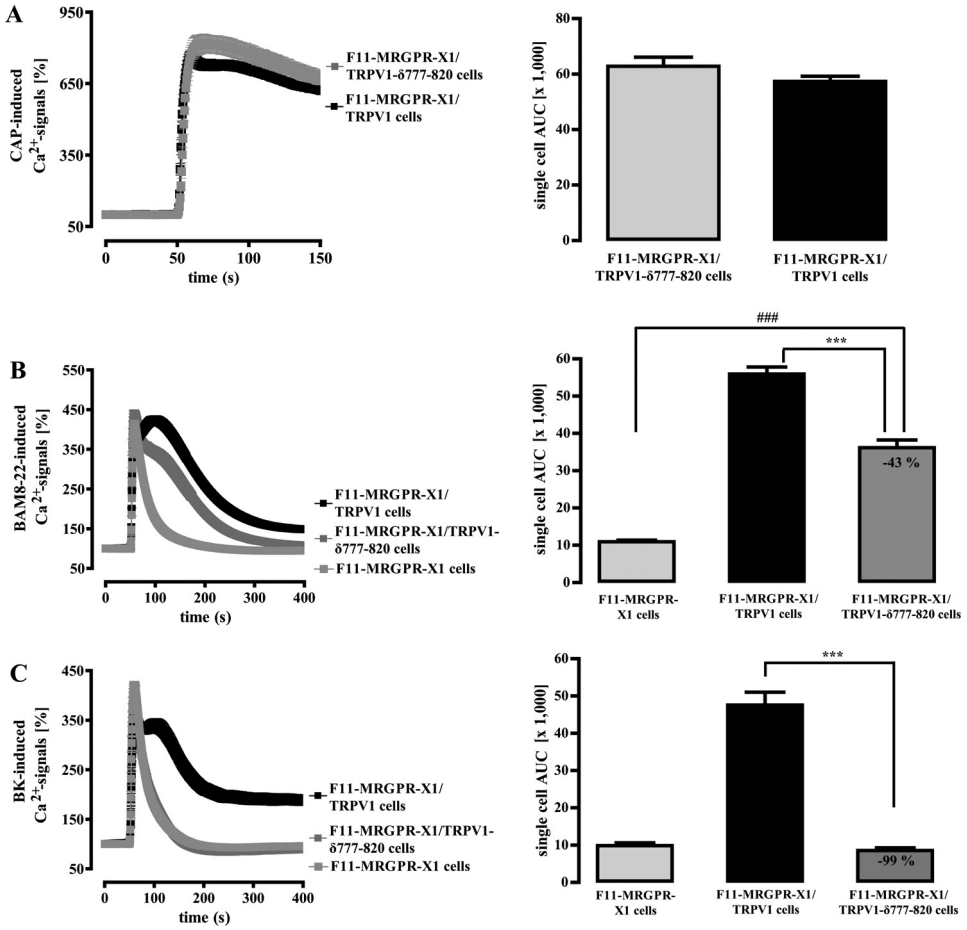

FIGURE 10. **MRGPR-X1-induced TRPV1 activation requires the PIP_2 binding site of the TRPV1.** Ca^{2+} signals in fura2-loaded F11-MRGPR-X1 cells and TRPV1-YFP or TRPV1-δ777–820-YFP co-expressing F11-MRGPR-X1 cells were monitored. CAP (10 nM, final) (*A*), BAM8–22 (2 μM, final) (*B*), and BK (100 nM, final) (*C*) were manually injected at time point 50 s. Data from 3–5 independent experiments were compiled, normalized by defining the first value (0.5 s) measured as 100%, and expressed as the mean ± S.E. The AUC for each measured cell was determined, data of all cells compiled, expressed as the mean ± S.E. and presented in *bar graphs*. *Asterisks* (***, $p < 0.001$) indicate a significant difference between TRPV1-δ777–820-YFP co-expressing F11-MRGPR-X1 and F11-MRGPR-X1/TRPV1 cells; *hash signs* (###, $p < 0.001$) between F11-MRGPR-X1 and TRPV1-δ777–820-YFP co-expressing F11-MRGPR-X1 cells.

Although TRPV1 sensitization to inflammatory stimuli such as heat and protons via G_q-induced PKC activation is widely recognized, little is known about direct TRPV1 activation as a consequence of G_q-dependent signaling independent of increased temperature and proton concentrations. So far, direct TRPV1 activation has been proposed for muscarinic-3 receptors (18) and metabotropic glutamate-5 receptors (55) via DAG production and for the B2R via PIP_2 degradation (17) or LOX activation (45). Herein, we noted that TRPV1 co-expression in F11-MRGPR-X1 cells profoundly enhanced MRGPR-X1-induced Ca^{2+} signals, Mn^{2+} influx, and cation currents at RT and constant pH, indicative of direct TRPV1 activation. Although PKC activity plays a dominant role in TRPV1 sensitization, it does not at all contribute to MRGPR-X1-induced TRPV1 activation. Because TRPV1 activation by MRGPR-X1 was independent from BAM8–22-induced Ca^{2+} release (Fig. 7) and resistant to chemical inhibition of PI3K, ERK-1/2, PKD, SRC, or LOX (Table 1 and Fig. 6), we postulate a significant role for PIP_2 and DAG in this process.

DAG-promoted channel activation has originally been described for members of the transient receptor potential cation channel C family but not for TRPV1 when expressed in Chinese hamster ovary cells (46). However, in rat DRG neurons OAG-induced calcium signals have been ascribed to increased TRPV1 activity (18, 55), indicating differential TRPV1 sensitivity to DAG in distinct cell lines. In DRG-derived F11 cells, we observed that accumulation of endogenous DAG and application of exogenous OAG induced Ca^{2+} signals solely in F11-MRGPR-X1/TRPV1, but not in F11-MRGPR-X1 cells, indicating that DAG activates TRPV1 in F11 cells. It has been reported that tyrosine 511 of TRPV1 is required for OAG-induced TRPV1 activation (18). In accord with the latter study, OAG-induced Ca^{2+} signals were almost completely abolished in TRPV1-Y511A expressing F11 cells. Because Ca^{2+} signals induced by high proton concentrations were unaltered in wild-type and TRPV1-Y511A expressing cells, we took advantage of this mutant to dissect the role of DAG in G_q-dependent TRPV1 activation. We observed that removal of the DAG binding site reduced MRGPR-X1-mediated TRPV1 activation by about 70%. Thus, we propose that DAG production is a major cellular event entailing MRGPR-X1-induced direct TRPV1 activation. Because DAG production also had a major impact on B2R-initiated TRPV1 activation, we assume that receptor induced DAG accumulation is of general sig-

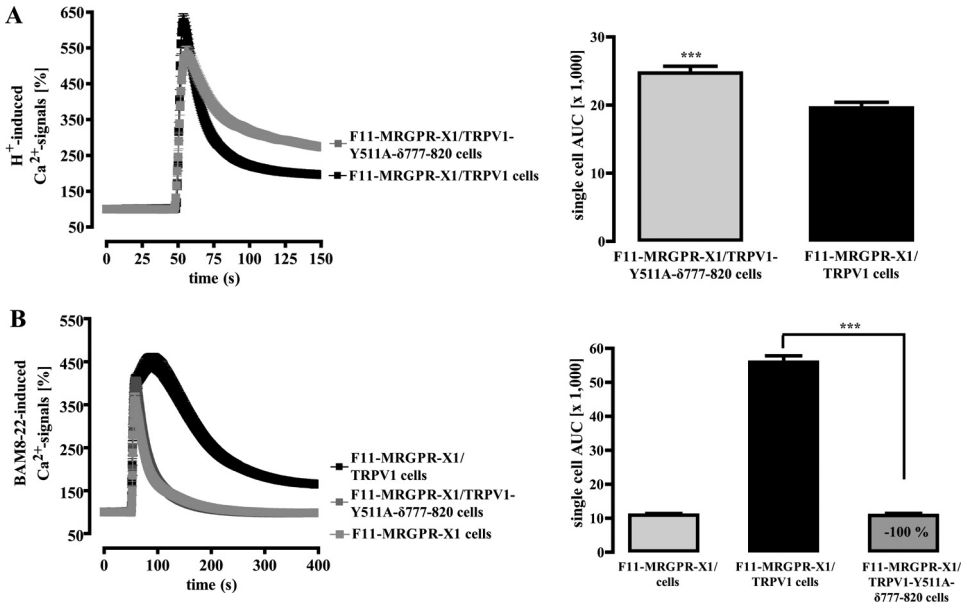

FIGURE 11. **DAG and PIP_2 are fully responsible for MRGPR-X1-induced TRPV1 activation.** Ca^{2+} signals in fura2-loaded F11-MRGPR-X1 cells and TRPV1-YFP or TRPV1-Y511A-δ777–820-YFP co-expressing F11-MRGPR-X1 cells were monitored. HCl (pH 5.0) (*A*) and BAM8–22 (2 μM, final) (*B*) were manually injected at time point 50 s. Data from 3–5 independent experiments were compiled, normalized by defining the first value (0.5 s) measured as 100%, and expressed as the mean ± S.E. The AUC for each measured cell was determined, and data of all cells were compiled, expressed as the mean ± S.E., and presented in *bar graphs*. *Asterisks* indicate a significant difference (***, $p < 0.001$) between F11-MRGPR-X1/TRPV1 and TRPV1-Y511A-δ777–820-YFP co-expressing F11-MRGPR-X1 cells.

nificance for TRPV1 activation by neuropeptides in DRG-derived F11 cells.

The PLC substrate PIP_2 has been reported to inhibit basal TRPV1 activity via binding to the C terminus of the channel protein. BK may, therefore, activate TRPV1 by relieving the ion channel from PIP_2 blockade (17, 19). However, PIP_2-mediated TRPV1 activation (15, 56) was also observed, and the role of PIP_2 degradation for TRPV1 activation has been questioned (10). In our experiments, deletion of the assumed PIP_2 binding site within TRPV1 (TRPV1-δ777–820) did not affect CAP-induced TRPV1 activation but completely abolished the effects of BK on TRPV1 activity. Of note, the TRPV1-δ777–820 mutant lacks serine 800, which is a major target of PKC-mediated TRPV1 sensitization. Because BK-promoted TRPV1 activation depended on PKC activity in F11 cells (Fig. 5*C*), reduced TRPV1-δ777–820 activation by BK may be independent of PIP_2. However, removal of the putative PIP_2 binding site also reduced BAM8–22-promoted TRPV1 activation, which does not rely on PKC activity (Figs. 2–4) and serine 800 (Fig. 3*E*). Thus, we propose that a second mechanism, most likely PIP_2 degradation, contributes to MRGPR-X1-mediated TRPV1 activation. This assumption is supported by the observation that the double mutant, TRPV1-Y511A-δ777–820, was not activated by MRGPR-X1 at all. Thus, it appears that a neatly orchestrated interplay between DAG binding and PIP_2 degradation regulates MRGPR-X1-induced TRPV1 activation independently from PKC.

A distinct role of PKC for MRGPR-X1-promoted TRPV1 sensitization as opposed to activation raises the question about underlying mechanisms. TRPV1 is a substrate of PKCα and PKCε (12). Although PKCα, a conventional PKC isoform, is activated by DAG and Ca^{2+}, PKCε belongs to the novel isoforms that critically depend on DAG but less on Ca^{2+} (57). Thus, BAM8–22-induced PLC activation may produce sufficient DAG to activate PKCε but may not release enough Ca^{2+} to activate PKCα. A further increase in $[Ca^{2+}]_i$ due to CAP-, proton-, or heat-induced TRPV1 activation may then additionally activate PKCα to sensitize TRPV1. However, additional studies are required to conclusively settle the issue as to differential impacts of distinct PKC isoforms on MRGPR-X1-promoted TRPV1 activation *versus* sensitization.

Despite the similarities found in MRGPR-X1- and B2R-promoted TRPV1 sensitization, we observed significant differences in direct TRPV1 activation. Although MRGPR-X1-induced TRPV1 activation is mainly mediated by DAG (71%) and PIP_2 (44%), B2R-promoted TRPV1 activation requires PKC activity (53%), DAG production (88%), PIP_2 degradation (99%), and LOX activity (44%). Overall, it appeared that diverging signaling pathways induced MRGPR-X1-promoted TRPV1 activation, whereas converging signaling pathways led to B2R-induced TRPV1 activation. Although at present the cellular and molecular mechanisms responsible for these differences remain elusive, they suggest that distinct G_q activating neuropeptides fine-tune TRPV1 activity differently in the same cellular context.

A major drawback for the use of TRPV1 blockers in clinical trials is increased core body temperature (10, 58). A recent study set out to correlate the effects of various TRPV1 blockers on heat- and proton-induced TRPV1 activation with their concomitant influence on body temperature in rats and mice. Hereby the authors revealed that TRPV1 blocker-induced hyperthermia is correlated with the propensity to inhibit proton-induced TRPV1 activation (59). Herein, we provide evidence suggesting that MRGPR-X1-induced sensitization of TRPV1 to protons can be differentiated from direct channel activation on the molecular level. Detailed knowledge about the molecular events leading to proton-independent TRPV1 activation via DAG and PIP_2 may be exploited to devise com-

pounds specifically targeting TRPV1-related pain without affecting body temperature.

In conclusion, we provide a thorough analysis of the functional interactions between MRGPR-X1 and TRPV1. We define a dual modulation of TRPV1 activity by MRGPR-X1 leading to PKC-dependent TRPV1 sensitization and DAG/PIP_2-mediated direct activation. These findings grant deeper insight into the molecular events underlying TRPV1-related pain syndromes in humans and further highlight the significance of MRGPR-X1 as putative therapeutic targets.

Acknowledgments—We thank Stephanie Hunger and Robin Meier for excellent technical assistance.

REFERENCES

1. Lembo, P. M., Grazzini, E., Groblewski, T., O'Donnell, D., Roy, M. O., Zhang, J., Hoffert, C., Cao, J., Schmidt, R., Pelletier, M., Labarre, M., Gosselin, M., Fortin, Y., Banville, D., Shen, S. H., Ström, P., Payza, K., Dray, A., Walker, P., and Ahmad, S. (2002) Proenkephalin A gene products activate a new family of sensory neuron, specific GPCRs. *Nat. Neurosci.* **5,** 201–209
2. Dong, X., Han, S., Zylka, M. J., Simon, M. I., and Anderson, D. J. (2001) A diverse family of GPCRs expressed in specific subsets of nociceptive sensory neurons. *Cell* **106,** 619–632
3. Breit, A., Gagnidze, K., Devi, L. A., Lagacé, M., and Bouvier, M. (2006) Simultaneous activation of the δ opioid receptor (δOR)/sensory neuron-specific receptor-4 (SNSR-4) hetero-oligomer by the mixed bivalent agonist bovine adrenal medulla peptide 22 activates SNSR-4 but inhibits δOR signaling. *Mol. Pharmacol.* **70,** 686–696
4. Solinski, H. J., Boekhoff, I., Bouvier, M., Gudermann, T., and Breit, A. (2010) Sensory neuron-specific MAS-related gene-X1 receptors resist agonist-promoted endocytosis. *Mol. Pharmacol.* **78,** 249–259
5. Burstein, E. S., Ott, T. R., Feddock, M., Ma, J. N., Fuhs, S., Wong, S., Schiffer, H. H., Brann, M. R., and Nash, N. R. (2006) Characterization of the Mas-related gene family. Structural and functional conservation of human and rhesus MrgX receptors. *Br. J. Pharmacol.* **147,** 73–82
6. Sikand, P., Dong, X., and LaMotte, R. H. (2011) BAM8–22 peptide produces itch and nociceptive sensations in humans independent of histamine release. *J. Neurosci.* **31,** 7563–7567
7. Chen, H., and Ikeda, S. R. (2004) Modulation of ion channels and synaptic transmission by a human sensory neuron-specific G-protein-coupled receptor, SNSR4/mrgX1, heterologously expressed in cultured rat neurons. *J. Neurosci.* **24,** 5044–5053
8. Davis, J. B., Gray, J., Gunthorpe, M. J., Hatcher, J. P., Davey, P. T., Overend, P., Harries, M. H., Latcham, J., Clapham, C., Atkinson, K., Hughes, S. A., Rance, K., Grau, E., Harper, A. J., Pugh, P. L., Rogers, D. C., Bingham, S., Randall, A., and Sheardown, S. A. (2000) Vanilloid receptor-1 is essential for inflammatory thermal hyperalgesia. *Nature* **405,** 183–187
9. Walker, K. M., Urban, L., Medhurst, S. J., Patel, S., Panesar, M., Fox, A. J., and McIntyre, P. (2003) The VR1 antagonist capsazepine reverses mechanical hyperalgesia in models of inflammatory and neuropathic pain. *J. Pharmacol. Exp. Ther.* **304,** 56–62
10. Vay, L., Gu, C., and McNaughton, P. A. (2012) The thermo-TRP ion channel family. Properties and therapeutic implications. *Br. J. Pharmacol.* **165,** 787–801
11. Tominaga, M., Wada, M., and Masu, M. (2001) Potentiation of capsaicin receptor activity by metabotropic ATP receptors as a possible mechanism for ATP-evoked pain and hyperalgesia. *Proc. Natl. Acad. Sci. U.S.A.* **98,** 6951–6956
12. Amadesi, S., Cottrell, G. S., Divino, L., Chapman, K., Grady, E. F., Bautista, F., Karanjia, R., Barajas-Lopez, C., Vanner, S., Vergnolle, N., and Bunnett, N. W. (2006) Protease-activated receptor 2 sensitizes TRPV1 by protein kinase Cε- and A-dependent mechanisms in rats and mice. *J. Physiol.* **575,** 555–571
13. Huang, J., Zhang, X., and McNaughton, P. A. (2006) Inflammatory pain. The cellular basis of heat hyperalgesia. *Curr. Neuropharmacol.* **4,** 197–206
14. Mandadi, S., Numazaki, M., Tominaga, M., Bhat, M. B., Armati, P. J., and Roufogalis, B. D. (2004) Activation of protein kinase C reverses capsaicin-induced calcium-dependent desensitization of TRPV1 ion channels. *Cell Calcium* **35,** 471–478
15. Stein, A. T., Ufret-Vincenty, C. A., Hua, L., Santana, L. F., and Gordon, S. E. (2006) Phosphoinositide 3-kinase binds to TRPV1 and mediates NGF-stimulated TRPV1 trafficking to the plasma membrane. *J. Gen. Physiol.* **128,** 509–522
16. Bhave, G., Hu, H. J., Glauner, K. S., Zhu, W., Wang, H., Brasier, D. J., Oxford, G. S., and Gereau, R. W., 4th (2003) Protein kinase C phosphorylation sensitizes but does not activate the capsaicin receptor transient receptor potential vanilloid 1 (TRPV1). *Proc. Natl. Acad. Sci. U.S.A.* **100,** 12480–12485
17. Chuang, H. H., Prescott, E. D., Kong, H., Shields, S., Jordt, S. E., Basbaum, A. I., Chao, M. V., and Julius, D. (2001) Bradykinin and nerve growth factor release the capsaicin receptor from PtdIns(4,5)P_2-mediated inhibition. *Nature* **411,** 957–962
18. Woo, D. H., Jung, S. J., Zhu, M. H., Park, C. K., Kim, Y. H., Oh, S. B., and Lee, C. J. (2008) Direct activation of transient receptor potential vanilloid 1(TRPV1) by diacylglycerol (DAG). *Mol. Pain* **4,** 42
19. Prescott, E. D., and Julius, D. (2003) A modular PIP2 binding site as a determinant of capsaicin receptor sensitivity. *Science* **300,** 1284–1288
20. Hellwig, N., Albrecht, N., Harteneck, C., Schultz, G., and Schaefer, M. (2005) Homo- and heteromeric assembly of TRPV channel subunits. *J. Cell Sci.* **118,** 917–928
21. Kleibeuker, W., Ledeboer, A., Eijkelkamp, N., Watkins, L. R., Maier, S. F., Zijlstra, J., Heijnen, C. J., and Kavelaars, A. (2007) A role for G protein-coupled receptor kinase 2 in mechanical allodynia. *Eur. J. Neurosci.* **25,** 1696–1704
22. Numazaki, M., Tominaga, T., Toyooka, H., and Tominaga, M. (2002) Direct phosphorylation of capsaicin receptor VR1 by protein kinase Cε and identification of two target serine residues. *J. Biol. Chem.* **277,** 13375–13378
23. Fan, S. F., Shen, K. F., and Crain, S. M. (1993) μ- and δ-opioid agonists at low concentrations decrease voltage-dependent K^+ currents in F11 neuroblastoma x DRG neuron hybrid cells via cholera toxin-sensitive receptors. *Brain Res.* **605,** 214–220
24. Fan, S. F., Shen, K. F., Scheideler, M. A., and Crain, S. M. (1992) F11 neuroblastoma x DRG neuron hybrid cells express inhibitory μ- and δ-opioid receptors which increase voltage-dependent K^+ currents upon activation. *Brain Res.* **590,** 329–333
25. Jow, F., He, L., Kramer, A., Hinson, J., Bowlby, M. R., Dunlop, J., and Wang, K. (2006) Validation of DRG-like F11 cells for evaluation of KCNQ/M-channel modulators. *Assay Drug Dev. Technol.* **4,** 49–56
26. Francel, P. C., Harris, K., Smith, M., Fishman, M. C., Dawson, G., and Miller, R. J. (1987) Neurochemical characteristics of a novel dorsal root ganglion X neuroblastoma hybrid cell line, F-11. *J. Neurochem.* **48,** 1624–1631
27. Jung, H., and Miller, R. J. (2008) Activation of the nuclear factor of activated T-cells (NFAT) mediates up-regulation of CCR2 chemokine receptors in dorsal root ganglion (DRG) neurons. A possible mechanism for activity-dependent transcription in DRG neurons in association with neuropathic pain. *Mol. Cell. Neurosci.* **37,** 170–177
28. Puttfarcken, P. S., Manelli, A. M., Arneric, S. P., and Donnelly-Roberts, D. L. (1997) Evidence for nicotinic receptors potentially modulating nociceptive transmission at the level of the primary sensory neuron. Studies with F11 cells. *J. Neurochem.* **69,** 930–938
29. McIlvain, H. B., Baudy, A., Sullivan, K., Liu, D., Pong, K., Fennell, M., and Dunlop, J. (2006) Pituitary adenylate cyclase-activating peptide (PACAP) induces differentiation in the neuronal F11 cell line through a PKA-dependent pathway. *Brain Res.* **1077,** 16–23
30. Boland, L. M., Allen, A. C., and Dingledine, R. (1991) Inhibition by bradykinin of voltage-activated barium current in a rat dorsal root ganglion cell line. Role of protein kinase C. *J. Neurosci.* **11,** 1140–1149
31. Rothe, K., Solinski, H. J., Boekhoff, I., Gudermann, T., and Breit, A. (2012) Morphine activates the E twenty six-like transcription factor-1/serum response factor pathway via extracellular signal-regulated kinases 1/2 in F11 cells derived from dorsal root ganglia neurons. *J. Pharmacol. Exp. Ther.*

342, 41–52
32. Li, Y., Ji, A., Weihe, E., and Schäfer, M. K. (2004) Cell-specific expression and lipopolysaccharide-induced regulation of tumor necrosis factor α (TNFα) and TNF receptors in rat dorsal root ganglion. *J. Neurosci.* **24,** 9623–9631
33. Gaudioso, C., Hao, J., Martin-Eauclaire, M. F., Gabriac, M., and Delmas, P. (2012) Menthol pain relief through cumulative inactivation of voltage-gated sodium channels. *Pain* **153,** 473–484
34. Eijkelkamp, N., Heijnen, C. J., Willemen, H. L., Deumens, R., Joosten, E. A., Kleibeuker, W., den Hartog, I. J., van Velthoven, C. T., Nijboer, C., Nassar, M. A., Dorn, G. W., 2nd, Wood, J. N., and Kavelaars, A. (2010) GRK2. A novel cell-specific regulator of severity and duration of inflammatory pain. *J. Neurosci.* **30,** 2138–2149
35. Fioravanti, B., De Felice, M., Stucky, C. L., Medler, K. A., Luo, M. C., Gardell, L. R., Ibrahim, M., Malan, T. P., Jr., Yamamura, H. I., Ossipov, M. H., King, T., Lai, J., Porreca, F., and Vanderah, T. W. (2008) Constitutive activity at the cannabinoid CB1 receptor is required for behavioral response to noxious chemical stimulation of TRPV1. Antinociceptive actions of CB1 inverse agonists. *J. Neurosci.* **28,** 11593–11602
36. Szallasi, A., Cortright, D. N., Blum, C. A., and Eid, S. R. (2007) The vanilloid receptor TRPV1. 10 years from channel cloning to antagonist proof-of-concept. *Nat. Rev. Drug Discov.* **6,** 357–372
37. Mizumura, K., Sugiura, T., Katanosaka, K., Banik, R. K., and Kozaki, Y. (2009) Excitation and sensitization of nociceptors by bradykinin. What do we know? *Exp. Brain Res.* **196,** 53–65
38. Cesare, P., Dekker, L. V., Sardini, A., Parker, P. J., and McNaughton, P. A. (1999) Specific involvement of PKC-ϵ in sensitization of the neuronal response to painful heat. *Neuron* **23,** 617–624
39. Moriyama, T., Iida, T., Kobayashi, K., Higashi, T., Fukuoka, T., Tsumura, H., Leon, C., Suzuki, N., Inoue, K., Gachet, C., Noguchi, K., and Tominaga, M. (2003) Possible involvement of P2Y2 metabotropic receptors in ATP-induced transient receptor potential vanilloid receptor 1-mediated thermal hypersensitivity. *J. Neurosci.* **23,** 6058–6062
40. Vellani, V., Mapplebeck, S., Moriondo, A., Davis, J. B., and McNaughton, P. A. (2001) Protein kinase C activation potentiates gating of the vanilloid receptor VR1 by capsaicin, protons, heat, and anandamide. *J. Physiol.* **534,** 813–825
41. Valenzano, K. J., Grant, E. R., Wu, G., Hachicha, M., Schmid, L., Tafesse, L., Sun, Q., Rotshteyn, Y., Francis, J., Limberis, J., Malik, S., Whittemore, E. R., and Hodges, D. (2003) *N*-(4-Tertiarybutylphenyl)-4-(3-chloropyridin-2-yl)tetrahydropyrazine-1(2H)-carbox-amide (BCTC), a novel, orally effective vanilloid receptor 1 antagonist with analgesic properties. I. *In vitro* characterization and pharmacokinetic properties. *J. Pharmacol. Exp. Ther.* **306,** 377–386
42. Plant, T. D., Zöllner, C., Kepura, F., Mousa, S. S., Eichhorst, J., Schaefer, M., Furkert, J., Stein, C., and Oksche, A. (2007) Endothelin potentiates TRPV1 via ETA receptor-mediated activation of protein kinase C. *Mol. Pain* **3,** 35
43. Turner, H., Fleig, A., Stokes, A., Kinet, J. P., and Penner, R. (2003) Discrimination of intracellular calcium store subcompartments using TRPV1 (transient receptor potential channel, vanilloid subfamily member 1) release channel activity. *Biochem. J.* **371,** 341–350
44. Zygmunt, P. M., Petersson, J., Andersson, D. A., Chuang, H., Sørgård, M., Di Marzo, V., Julius, D., and Högestätt, E. D. (1999) Vanilloid receptors on sensory nerves mediate the vasodilator action of anandamide. *Nature* **400,** 452–457
45. Shin, J., Cho, H., Hwang, S. W., Jung, J., Shin, C. Y., Lee, S. Y., Kim, S. H., Lee, M. G., Choi, Y. H., Kim, J., Haber, N. A., Reichling, D. B., Khasar, S., Levine, J. D., and Oh, U. (2002) Bradykinin-12-lipoxygenase-VR1 signaling pathway for inflammatory hyperalgesia. *Proc. Natl. Acad. Sci. U.S.A.* **99,** 10150–10155
46. Hofmann, T., Obukhov, A. G., Schaefer, M., Harteneck, C., Gudermann, T., and Schultz, G. (1999) Direct activation of human TRPC6 and TRPC3 channels by diacylglycerol. *Nature* **397,** 259–263
47. Ryu, S., Liu, B., Yao, J., Fu, Q., and Qin, F. (2007) Uncoupling proton activation of vanilloid receptor TRPV1. *J. Neurosci.* **27,** 12797–12807
48. Gavva, N. R., Tamir, R., Klionsky, L., Norman, M. H., Louis, J. C., Wild, K. D., and Treanor, J. J. (2005) Proton activation does not alter antagonist interaction with the capsaicin-binding pocket of TRPV1. *Mol. Pharmacol.* **68,** 1524–1533
49. Choi, S. S., and Lahn, B. T. (2003) Adaptive evolution of MRG, a neuron-specific gene family implicated in nociception. *Genome Res.* **13,** 2252–2259
50. Tay, S. K., Blythe, J., and Lipovich, L. (2009) Global discovery of primate-specific genes in the human genome. *Proc. Natl. Acad. Sci. U.S.A.* **106,** 12019–12024
51. Hao, L., Ge, X., Wan, H., Hu, S., Lercher, M. J., Yu, J., and Chen, W. H. (2010) Human functional genetic studies are biased against the medically most relevant primate-specific genes. *BMC Evol. Biol.* **10,** 316
52. Grazzini, E., Puma, C., Roy, M. O., Yu, X. H., O'Donnell, D., Schmidt, R., Dautrey, S., Ducharme, J., Perkins, M., Panetta, R., Laird, J. M., Ahmad, S., and Lembo, P. M. (2004) Sensory neuron-specific receptor activation elicits central and peripheral nociceptive effects in rats. *Proc. Natl. Acad. Sci. U.S.A.* **101,** 7175–7180
53. Han, S. K., Dong, X., Hwang, J. I., Zylka, M. J., Anderson, D. J., and Simon, M. I. (2002) Orphan G protein-coupled receptors MrgA1 and MrgC11 are distinctively activated by RF-amide-related peptides through the $G\alpha_{q/11}$ pathway. *Proc. Natl. Acad. Sci. U.S.A.* **99,** 14740–14745
54. Daaka, Y., Luttrell, L. M., Ahn, S., Della Rocca, G. J., Ferguson, S. S., Caron, M. G., and Lefkowitz, R. J. (1998) Essential role for G protein-coupled receptor endocytosis in the activation of mitogen-activated protein kinase. *J. Biol. Chem.* **273,** 685–688
55. Kim, Y. H., Park, C. K., Back, S. K., Lee, C. J., Hwang, S. J., Bae, Y. C., Na, H. S., Kim, J. S., Jung, S. J., and Oh, S. B. (2009) Membrane-delimited coupling of TRPV1 and mGluR5 on presynaptic terminals of nociceptive neurons. *J. Neurosci.* **29,** 10000–10009
56. Sowa, N. A., Street, S. E., Vihko, P., and Zylka, M. J. (2010) Prostatic acid phosphatase reduces thermal sensitivity and chronic pain sensitization by depleting phosphatidylinositol 4,5-bisphosphate. *J. Neurosci.* **30,** 10282–10293
57. Poole, A. W., Pula, G., Hers, I., Crosby, D., and Jones, M. L. (2004) PKC-interacting proteins. From function to pharmacology. *Trends Pharmacol. Sci.* **25,** 528–535
58. Gavva, N. R., Bannon, A. W., Surapaneni, S., Hovland, D. N., Jr., Lehto, S. G., Gore, A., Juan, T., Deng, H., Han, B., Klionsky, L., Kuang, R., Le, A., Tamir, R., Wang, J., Youngblood, B., Zhu, D., Norman, M. H., Magal, E., Treanor, J. J., and Louis, J. C. (2007) The vanilloid receptor TRPV1 is tonically activated *in vivo* and involved in body temperature regulation. *J. Neurosci.* **27,** 3366–3374
59. Garami, A., Shimansky, Y. P., Pakai, E., Oliveira, D. L., Gavva, N. R., and Romanovsky, A. A. (2010) Contributions of different modes of TRPV1 activation to TRPV1 antagonist-induced hyperthermia. *J. Neurosci.* **30,** 1435–1440